AN INVESTIGATION OF A MODIFIED COLLOID MILL FOR PIGMENT DISPERSION

A THESIS

Presented to

the Faculty of the Graduate Division

Georgia Institute of Technology

In Partial Fulfillment

of the Requirements for the Degree

Master of Science in Chemical Engineering

By

William Raymond Tooke, Jr.

March 1955

AN INVESTIGATION OF A MODIFIED COLLOID

MILL FOR PIGMENT DISPERSION

Approved:

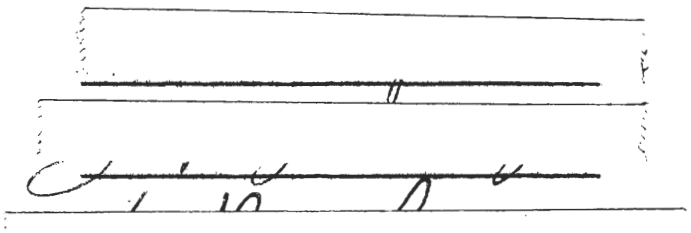

Date Approved by Chairman: April 11, 1955

PREFACE

Over a period of several years the author has been engaged in numerous research and development projects related to the protective coatings industry. As a result of these contacts, a continuing interest in the technical problems of this industry has been acquired.

The entry of the industrial chemist into the field of coatings technology is generally regarded as the milestone that marked the beginning of the modern paint industry. Yet the subsequent engineering development of high-speed production equipment deserves credit for making available to the public the products of the chemist's skill. However, from the theoretical standpoint, the technical operation of pigment dispersion is still woefully inefficient. The present work represents what is believed to be a new and fundamental approach to the design of high-speed milling equipment of the colloid mill type.

The author is particularly grateful to Dr. H. C. Lewis for guidance in the theoretical and experimental work and for editorial assistance with the manuscript. The cooperation of Dr. Frederick Bellinger and the Georgia Tech Engineering Experiment Station in making available funds for the fabrication of experimental equipment is also gratefully acknowledged.

TABLE OF CONTENTS

TABLE OF CONTENTS (Continued)

LIST OF TABLES

LIST OF FIGURES

AN INVESTIGATION OF A MODIFIED COLLOID MILL FOR PIGMENT DISPERSION

SUMMARY

A theoretical and experimental investigation was undertaken to explore the feasibility of a fundamentally new design for pigment-dispersion equipment.

The equipment is essentially a colloid mill embodying a unique combination of counter-centrifugal flow of the liquid to be milled under an external applied pressure, and continuous internal classification of pigment particle size to effect the discharge of a paste of the desired "fineness of grind".

An extensive literature and patent search indicated that the proposed combination of physical principles was novel for pigment-dispersion applications. Thereupon, a theoretical analysis of fluid flow in the equipment was undertaken. A rigorous theoretical treatment was beyond the scope of the present work, but the approximations developed supported previous intuitive hypotheses.

On the basis of the theoretical information available, a prototype mill was designed and constructed. The frame of a Model 1402 Morehouse Mill was used as an advanced starting point. The Morehouse Mill was fitted with a completely new rotor, stator, head, and other auxiliaries required to effect the new design principles.

Two series of experimental studies of the equipment were made. The first series was primarily aimed at exploring the flow characteristics of the mill, and the second at evaluating the pigment dispersion potentials of the equipment. The flow experiments served the intended purpose but only qualitatively supported the theoretical hydrodynamics. The dispersion studies demonstrated unsatisfactory performance for this initial design. Inadequate "grinds" and a tendency for the mill to overheat were the shortcomings. Proposals for correcting these defects include the substitution of carborundum milling faces for the plain steel faces of the present design and the addition of a water jacket on the head of the mill to improve heat transfer.

It is concluded that the new colloid mill design embodies patentable novelty, that the theoretical hydrodynamics as developed are only qualitatively applicable, that the initial experimental equipment is unsatisfactory from the standpoint of dispersion and overheating, but that the ultimate potentials of the design have not been realized in the present work.

CHAPTER I

INTRODUCTION

> I am a part of all that I have met;
> Yet all experience is an arch wherethro'
> Gleams that untravelled world, whose margin fades
> Forever and forever when I move.†

Fine-particle dispersion.--The unit operation of fine-particle or pigment dispersion has never received widespread attention from chemical engineers. Nevertheless, in the manufacture of paints, rubber goods, plastics, ceramics, and numerous minor products, this unit operation is fundamental. Since the object of the present work was to investigate a mechanical device for producing fine-particle dispersion, a summary discussion of the mechanisms involved is pertinent.

In the paint industry, pigment dispersion is referred to as "grinding". This is really a misnomer that stems from the historical practice of grinding and reducing coarse solid materials in oils to produce paints. Modern pigments as supplied to paint manufacturers are generally of such fineness in particle size that none of the grinding equipment normally used is capable of further reducing the individual particles. The term "pigment dispersion" is more appropriate to the actual operation.

Modern dry pigments usually have average particle sizes of less than one micron in diameter. Extensive data on particle size

---

†From the poem "Ulysses" by Alfred Lord Tennyson.

measurements on pigments have been compiled by Fischer (1). The surface area of these materials is quite large, and this surface is covered with a layer of air or other adsorbed gases. The work of pigment dispersion involves breaking up large clusters of these fine particles and displacing the gas-pigment interface with a vehicle-pigment interface. In most cases, no actual crushing of individual particles occurs. Moreover, the wetting of pigments by vehicle liquids is usually spontaneous and accompanied by the liberation of a perceptible amount of heat. Harkins and Dahlstrom (2) have measured heats of immersion of pigment-type materials in various liquids. "Wettability" as manifested by heats of immersion assists in the pigment dispersion operation so that theoretically only the work for reduction of persistent pigment agglomerates is required. From this point of view, current practice of pigment dispersion is very inefficient, since the actual energy required greatly exceeds the theoretical energy requirement for reducing the agglomerates.

Dispersion equipment.--An examination of the operation of various types of dispersion equipment readily indicates the causes of energy dissipation. The dispersion action in any type of equipment occurs by one or more of the following mechanisms:

(1) Crushing - Agglomerates are crushed between co-acting surfaces.

(2) Shear - Fluid shear within the mass of the vehicle disintegrates pigment agglomerates.

(3) Impact - Agglomerates are dispersed kinetically by the effects of sudden accelerations and decelerations. In each case, only a

portion of the energy expended in the vehicle is effective in agglomerate reduction. The greater part of this energy must be used in overcoming the viscous resistance of the vehicle, with resultant generation of heat.

Descriptions of dispersion equipment are presented in Perry's Engineers' Handbook (3), and more detailed discussions of this subject have been given by Fischer (4) and by Bidlack and Fasig (5). These references also contain extensive bibliographies. Sufficient background for the present thesis is provided by a brief comparison of the operation of the ball mill, the roll mill, and the high-speed stone mill.

Ball mills are extensively used in pigment-dispersion work; they are characterized by simplicity of operation and the ability to produce almost any desired degree of dispersion. Skillful operators are not required. The mill is simply loaded, allowed to run the requisite length of time, and the dispersed product is then discharged. The primary disadvantages are that batch sizes are limited to the capacity of the mill, and cleanup for a changeover in products is time-consuming.

Dispersion in a ball mill results from the cascading action of the ball charge as the mill turns. Crushing action between the individual balls is the main dispersion mechanism; however, fluid shear contributes significant effects. Impact, in the sense of the foregoing definition, is an insignificant mechanism.

Numerous types of roll mills have been developed. Currently, roll mills having one, two, three, and five rolls are used in various industries. By far the most popular mill of this type for pigment dispersion operations in the paint industry is the three-roll mill.

Before dispersing pigments in a roll mill, it is necessary to prepare a heavy pigment-vehicle paste. For this operation, pigments are combined with the vehicle in a paste mixer designed for this purpose. The paste mixer is similar in operation to a dough mixer. The thick paste so prepared is fed into the hopper of the roll mill.

Two mechanisms are involved in roll-mill dispersion. Large agglomerates are crushed mechanically between the rolls, while agglomerates smaller than the roll separation are dispersed by fluid shear created by differential roll speeds. The shearing mechanism predominates in the production of dispersions on this equipment.

Ease of cleaning is one marked advantage of the roll mill. Thus, it is capable of handling a variety of products and batch sizes with efficiency. Very excellent dispersions can be produced on this equipment. The roll mill is capable of grinding much thicker pastes than are suitable for the ball mill. The disadvantages of the roll mill are that it requires the continuous attention of a skilled operator, the use of volatile vehicles is not usually practical, and a premixed charge to the mill is necessary.

The high-speed stone mill is a more recently developed type of dispersion equipment which combines features of the colloid mill and the now-obsolete stone mill. The "stones" are actually precision formed from silicon carbide and are usually disc-shaped. The material to be milled is fed to the grinding faces through a large central hole in the stator stone. The pumping action of the rotor turning at about 3600 rpm drives the material rapidly through the milling zone between the stones

in a centrifugal spiral path and discharges it at the periphery. The stones may be set at clearances as small as 0.001 inch, but they are never allowed actually to come into grinding contact.

Like the roll mill the high-speed stone mill requires a paste premix of raw materials prior to the milling operation. Indeed, the premix to this mill must be of a much lower viscosity than is desirable for the roll mill. Similarly, the use of highly volatile solvents may be impractical. In the past, it had been thought that this equipment was incapable of producing acceptable products of the gloss-enamel type, but more recently finely ground enamels have been prepared by careful attention to technique. Practical performance data on this subject have been reported by Foy et al. (6) and by Taylor (7). Currently, however, the high-speed stone mill finds its major application in the preparation of house paints and other products not requiring the finest dispersion. A tendency for these mills to run hot is another factor that mitigates against very fine grinding.

Advantages of the high-speed stone mills are that they occupy very little floor space and are comparatively low in cost. Furthermore they are unequaled in their capacity for production of paints not requiring the finest grinds; and while they do require some attention from an operator, they are far less critical in this respect than roll mills.

The dispersion action of the high-speed stone mill results largely from fluid shear between the closely set milling faces. At the same time, kinetic impact of pigment particles against the gritty stones

must certainly contribute to the dispersive effects. Inasmuch as the stones do not come into direct contact, crushing action on agglomerates should occur relatively infrequently if the premix is properly prepared.

At the present time, virtually all paints manufactured are processed on one of the three types of mills that have been described. The fundamental design of this equipment has remained unchanged for many years, although there have been improvements in mechanical details from time to time. Several years ago a new type of mill was introduced to the industry. This equipment, known as the Kady mill (8), has gained some acceptance by the trade. Essentially, it is a large-scale rotary homogenizer which disperses by a combination of high-speed fluid shear and impact. Researches by the Scientific Section of the National Paint, Varnish, and Lacquer Association further attest to current interest in equipment design. Studies of a modification of the three-roll mill and more recently a new design for the high-speed stone mill have been reported by Shurts (9). Large potentials for improvements in equipment design are recognized.

Development of the colloid mill.--The equipment investigated in the present work was a modified type of colloid mill. Historically, the original concept of the colloid mill dates back to the turn of the century. In his monograph on this subject, Travis (10) states that little attention was given to papers published in Russia in the 1900's on fine grinding equipment but that von Weimarn (11), a Russian, deserves credit for publication of a conception of a mill of this type in 1910.

Despite this fact, the invention of the colloid mill has been generally attributed to Plauson (12), who, in 1921, applied for patents on his design. On the heels of his patents, a number of papers published in trade and technical journals quickly brought this equipment to the attention of the chemical process industries. Since that time, numerous designs of colloid mills have been proposed and patented. Clayton (13) has given a review of commercially available types, and Fischer (14) has supplemented this with a presentation of more current information. A chronological listing of pertinent patents in this field has been compiled (15).

A careful study of the foregoing references has lead to the following generalizations:

(1) In most colloid mills, the feed enters at a point near the axis of rotation and centrifugal force aids in moving the material through the milling zone.

(2) The milling faces of most colloid mills are either discs, truncated cones, or a combination of these.

(3) Without exception, when the milling faces are truncated cones, the rotor is the inner or solid milling element.

(4) Only one type of colloid mill has been designed to drive material through the milling zone in a centripetal direction, and this mill utilizes either disc or ring labyrinth-shaped milling faces.

Against these established design features, the fundamental novelty of any proposed design modification must be tested.

CHAPTER II

HYDRODYNAMICS OF A MODIFIED MILL

Design principles.--This thesis proposes a design modification of the colloid mill that is intended to effect an integration of the two distinct unit operations of dispersion and centrifugal internal classification of solid particles in a liquid medium into a single mechanical operation. The essential features of the new design are best illustrated by reference to the mill assembly drawing of Figure 1. The liquid or paste material to be milled is introduced into a hopper (A) directly above a small variable rate pump or feeder (B). This pump forces the material into the cavity (C) surrounding the rotor (D). The rotor is driven through the shaft (E) by a motor (F). The material in the cavity (C) is forced under pressure from the pump (B) into the milling and classifying zone (G) between the rotor (D) and the stator (H). The milled and classified product leaves the milling and classifying zone (G) through an annular space (J) between the stator (H) and the shaft (E) and passes down and out of the mill through the duct (K). The water jacket (L) serves to cool the mill.

This mill is intended to be distinguished from conventional colloid mills by its capacity for effecting continuous internal classification of particle sizes of the pigment agglomerates. Under actual operating conditions, this means that particles of a given size will assume a more or less static position in the milling zone with respect to radial

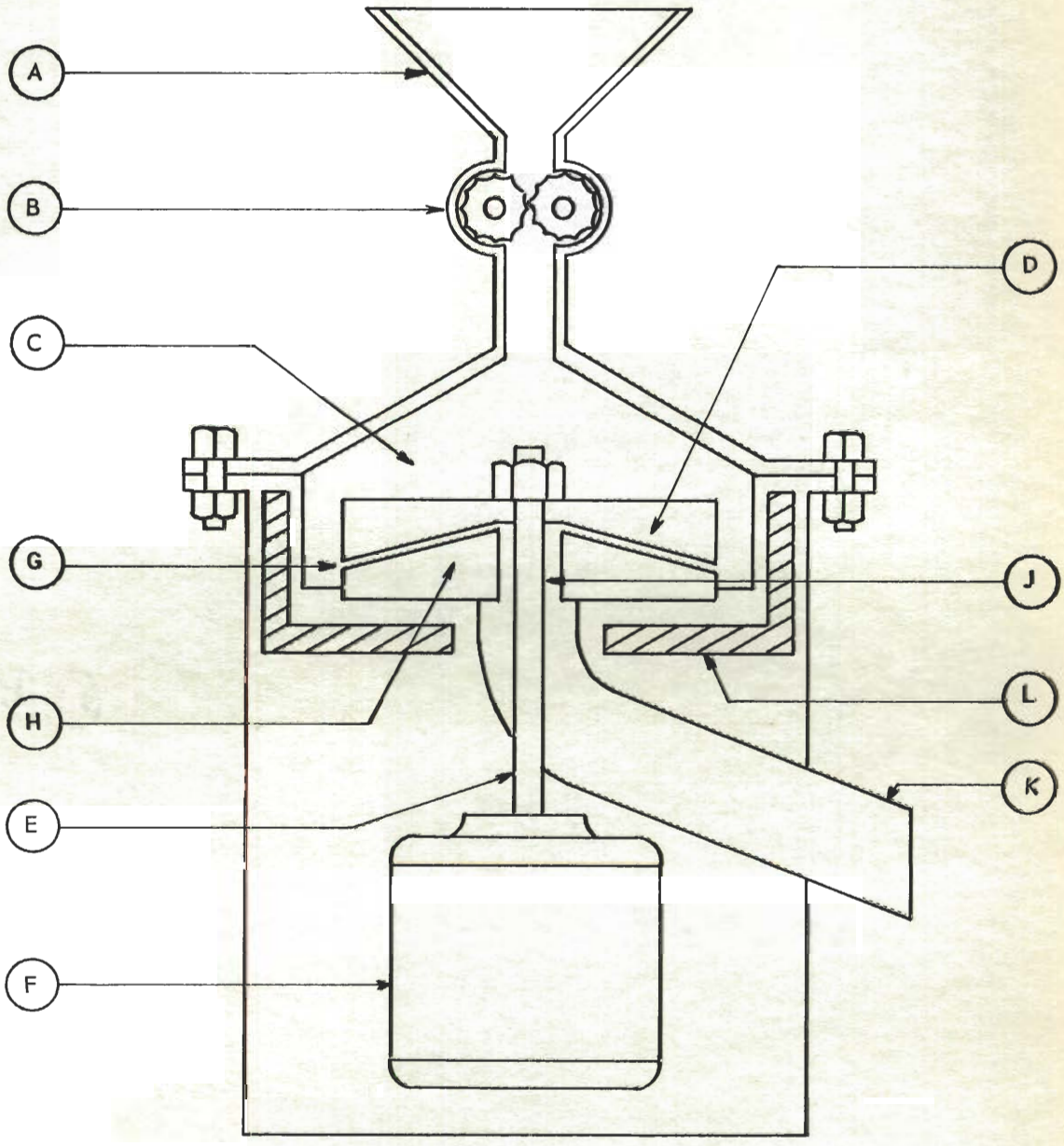

Figure 1. Mill Assembly.

movement--this static position resulting from a dynamic balancing of centrifugal force against an equal and opposite fluid pressure force. As the agglomerate particles are broken down by shearing forces, the resulting fragments of the desired fineness should be displaced toward the stator and centripetally up the stator and finally out of the milling zone at the annular space.

Power requirements.--A means of calculating the theoretical power requirements of the mill has been developed based on the following assumptions:

1. Fluid flow between the milling faces in the direction of rotation is laminar, and the angular velocity profile of the fluid is in the form of a straight line with zero angular velocity at the stator and maximum angular velocity at the rotor.

2. The viscosity does not vary with the rate of shear, and the temperature is uniform in the milling zone.

The validity of these assumptions for practical applications will depend on the properties of the fluid and the construction of the mill. Obviously, the Reynolds number must be below the critical value throughout the milling zone, and the fluid must be neither dilatent nor thixotropic. Specific applicability to the actual equipment will be discussed in Chapter III.

The essential geometry of the mill together with pertinent dimensional notation is shown in Figure 2. The "Table of Symbols" in Appendix A is applicable to all derivations. The approximate expression for theoretical power requirements is derived as follows:

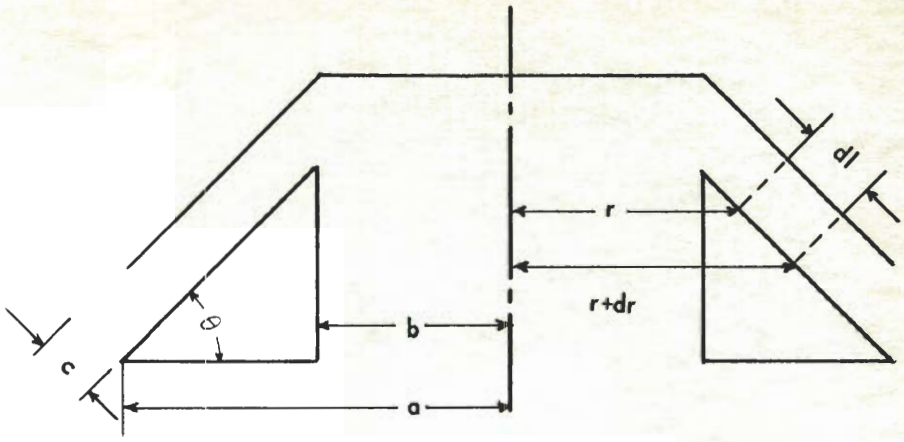

Figure 2. Geometry and Notation.

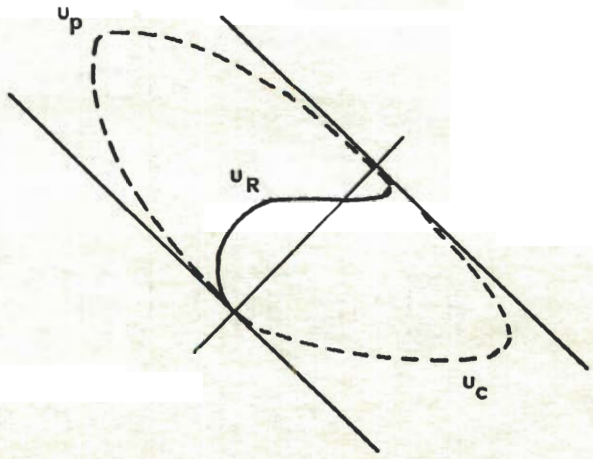

Figure 3. Velocity Profiles.

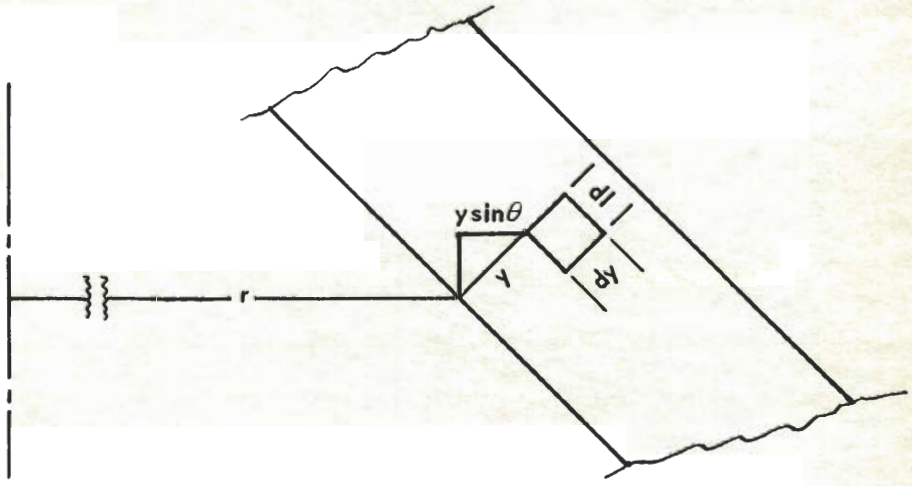

Figure 4. Free Body Diagram.

$$\frac{dr}{dl} = \cos\theta$$

$$dl = \frac{dr}{\cos\theta}$$

$$dA = \frac{2\pi r dr}{\cos\theta}$$

$$\frac{dF}{dA} = \frac{zV}{c} \quad \text{(Newton's law of viscosity)}$$

The circumferential velocity is therefore given by the expression:

$$V = R(2\pi r)$$

$$dF = \frac{zR(2\pi r)(2\pi r dr)}{c\cos\theta}$$

$$dP = (dF)(2\pi r R)$$

$$= \frac{zR^2(2\pi r)^3 dr}{c\cos\theta}$$

$$P = \frac{8\pi^3 zR^2}{c\cos\theta}\int_b^a r^3 dr = \frac{8\pi^3 zR^2}{c\cos\theta}\left[\frac{r^4}{4}\right]_b^a$$

$$P = \frac{2\pi^3 zR^2(a^4 - b^4)}{c\cos\theta} \qquad (1)$$

Attention is directed to the fact that equation (1) does not include all sources of power losses resulting from fluid friction. Specifically, the friction at the dy faces of the free body of Figure 4 has been ignored. Obviously this is not a significant omission since the change in circumferential velocity in the $\underline{l}$ direction, $\frac{du}{dl}$, is negligible as compared to the change in the $\underline{c}$ direction, $\frac{du}{dc}$. The friction resulting from radial fluid flow and the friction on the top of the rotor are also ignored as relatively minor losses.

Fluid flow.--A completely rigorous analysis of fluid flow in this equipment is beyond the scope of the present investigation. Furthermore, the partial analysis here presented is confined to homogeneous fluids. Nevertheless, the capacity of the modified mill to develop the unique flow pattern here described is the primary feature of the design.

First, a qualitative approach is of interest. For the purpose of this analysis, only the components of flow in the centripetal or radial direction will be considered. The velocity profile of a Newtonian fluid flowing between two stationary parallel plates is in the form of a parabola (16). To a good first approximation, the concentric cones of the modified mill may be regarded as parallel plates. Thus, if the rotor of the mill remains stationary, external fluid pressure will force the fluid through the milling zone in a centripetal direction, producing a parabolic velocity profile as represented by the dotted line, u_p, in Figure 3. On the other hand, if the rotor were turning and if the fluid were introduced at the central annulus at just a sufficient rate to maintain the milling zone full of fluid, then another velocity profile, u_c, in the opposite direction would obtain with the fluid discharging to atmospheric pressure at the periphery. The general shape of this velocity profile must be as shown in Figure 3, with zero velocity at each solid surface and a skewing of maximum velocity toward the rotor as a result of the centrifugal pumping action of the moving rotor. A more quantitative development of this shape will be given later. Finally, if one considers the combined effects produced by the mill in normal operation, the resultant velocity profile, u_R, is obtained. For a given fluid, the exact

form of this curve will be determined by the selected position of the datum line between the periphery and the annulus and by the previously mentioned dynamic balancing of the centrifugal effect against the externally applied fluid pressure.

A mathematical approach to this fluid flow problem has been partially developed, based on the principles of fluid mechanics. A free-body diagram of the system is presented in Figure 4. The differential element of fluid may be visualized as a thin ring located at a distance, y, from the stator.

A completely rigorous treatment of this problem would involve solution of the force equations in the $\underline{l}$ and $\underline{y}$ directions together with the continuity equation. An examination of these equations appears to indicate that this is a suitable subject for a mathematical thesis and, accordingly, beyond the scope of the present study. Nevertheless, some insight into the fluid flow in this equipment can be gained by a simplified mathematical treatment involving admittedly broad assumptions.

As in the calculation of power requirements, assume that the angular velocity profile is a straight line and therefore:

$$\omega = \frac{y}{c}\,\omega_R. \qquad (2)$$

Forces in the $\underline{l}$ direction are summed up as follows:

$$s\ 2\pi(r + y \sin\theta)^2 \left(\frac{y^2\omega_R^2}{c^2}\right) dydl \cos\theta \text{ (centrifugal)}$$

$$- 2\pi(r + y \sin\theta)\left(\frac{\partial p}{\partial l}\right) dydl \text{ (pressure)}$$

$$+ 2\pi(r + y \sin\theta)z\left(\frac{\partial^2 u}{\partial y^2}\right) dydl \text{ (shear)}$$

$$= 0. \qquad (3)$$

Acceleration in the $\underline{l}$ direction has been assumed to be negligible compared to the other terms.

Upon simplifying and rearranging, one obtains

$$\frac{\partial p}{\partial l} = \frac{sry^2\omega_R^2 \cos\theta}{c^2} + \frac{sy^3\omega_R^2 \sin\theta \cos\theta}{c^2} + z\left(\frac{\partial^2 u}{\partial y^2}\right) \qquad (4)$$

$$\frac{\partial^2 u}{\partial y^2} = -\frac{sry^2\omega_R^2 \cos\theta}{zc^2} - \frac{sy^3\omega_R^2 \sin\theta \cos\theta}{zc^2} + \frac{1}{z}\frac{\partial p}{\partial l}. \qquad (5)$$

If one assumes that $\frac{\partial p}{\partial l}$ is not a function of $\underline{y}$, then equation (5) may be integrated to give:

$$\frac{\partial u}{\partial y} = -\frac{sr\omega_R^2 \cos\theta\, y^3}{3\,zc^2} - \frac{s\omega_R^2 \sin\theta \cos\theta\, y^4}{4\,zc^2} + \frac{1}{z}\frac{\partial p}{\partial l} y + A \qquad (6)$$

$$u = -\frac{sr\omega_R^2 \cos\theta\, y^4}{12\,zc^2} - \frac{s\omega_R^2 \sin\theta \cos\theta\, y^5}{20\,zc^2} + \frac{1}{2z}\frac{\partial p}{\partial l} y^2 + Ay + B. \qquad (7)$$

Since the velocity at the boundaries must be zero,

when

$$y = 0,\ u = 0 = B$$

and when

$$y = c,\ u = 0 = -\frac{sr\omega_R^2 \cos\theta\, c^4}{12\, zc^2} - \frac{s\omega_R^2 \sin\theta \cos\theta\, c^5}{20\, zc^2} + \frac{\partial p}{\partial l}\frac{c^2}{2z} + A_c.$$

Upon substituting the values obtained for the constants in equation (7), one obtains

$$u = \frac{sr\omega_R^2 \cos\theta\,(c^3y - y^4)}{12\, zc^2} + \frac{s\omega_R^2 \sin\theta \cos\theta\,(c^4y - y^5)}{20\, zc^2}$$

$$- \frac{1}{2z}\frac{\partial p}{\partial l}(cy - y^2). \qquad (8)$$

This is the equation for the velocity profile in the l direction.

The equation for flow, Q, may be developed as follows:

$$dQ = udA = u\, 2\pi r dy \qquad (9)$$

and substituting the expression for u from equation (8) one obtains

$$dQ = \frac{2\pi r^2 s\omega_R^2 \cos\theta\,(c^3y - y^4)dy}{12\, zc^2} + \frac{2\pi r s\omega_R^2 \sin\theta \cos\theta(c^4y - y^5)dy}{20\, zc^2}$$

$$- \frac{2\pi r}{2z}\frac{\partial p}{\partial l}(cy - y^2)dy. \qquad (10)$$

Integration of this expression with respect to y between the limits θ and c upon simplification yields:

$$Q = \frac{\pi r^2 s\omega_R^2(\cos\theta)c^3}{20\, z} + \frac{\pi r s\omega_R^2 \sin\theta(\cos\theta)c^4}{30\, z} - \frac{\pi r}{6z}\frac{\partial p}{\partial l}c^3. \qquad (11)$$

Pressure drop may be calculated by rearranging equation (11) into the form

$$\frac{\partial p}{\partial l} = \frac{3rs\omega_R^2 \cos\theta}{10} + \frac{s\omega_R^2 \sin\theta(\cos\theta)c}{5} - \frac{6zQ}{\pi rc^3} . \qquad (12)$$

And since $dr = dl \cos\theta$, then

$$\partial p = \frac{3rs\omega_R^2 dr}{10} + \frac{s\omega_R^2(\sin\theta)cdr}{5} - \frac{6zQdr}{\pi(\cos\theta)c^3 r} . \qquad (13)$$

Finally, if $\underline{Q}$ is taken as a constant, integration with respect to $\underline{r}$ gives

$$p = \frac{s\omega_R^2}{20}[4c \sin\theta(r_1 - r_2) + 3(r_1^2 - r_2^2)] - \frac{6zQ}{\pi c^3 \cos\theta} \ln\frac{r_1}{r2} . \qquad (14)$$

It is hoped that the mathematically minded reader will forgive the rather tenuous assumptions and the liberties taken with partial derivatives in this attempt at an approximate analysis of the flow phenomena. Further, it is hoped that such readers may become interested in developing a rigorous solution. The foregoing analysis is justified, first, because it supports the intuitive flow visualization, and second, because it provides a guide to the correlation of experimental data.

Specifically, observe that the velocity profile expression of equation (8) contains three terms. The first two terms describe the centrifugal effect, and the power forms in $\underline{y}$ are similar to the shape described for V_c in Figure 3. Moreover, the third term is parabolic as described for the pressure component, shown as V_p in Figure 3. The utility of this concept for data correlation will be demonstrated in Chapter VI.

Combined effects on suspended particles.--In most practical applications for this equipment, the fluid to be milled is actually a thin paste. The total pigment solids in the paste may vary from about 5 to 50 per cent, and these solids are initially in the form of particle agglomerates of various sizes. The treatment of this complex system, as presented here, is largely descriptive in nature.

Particle size classification in the modified mill occurs under the influence of centrifugal force. The magnitude of this force is expressed by the equation

$$F = \frac{w}{g} r\omega^2 \qquad (15)$$

where

F = centrifugal force in grams,
w = weight of particle in grams,
g = acceleration of gravity in cm/sec^2,
r = radius of curvature in cm, and
ω = angular velocity in radians/sec.

As an approximation assume that Stokes's law for settling particles is applicable. Then

$$V_s = \frac{d^2}{18z} (s_p - s_l) r\omega^2 \qquad (16)$$

where

V_s = velocity of settling in cm/sec,
d = effective diameter of particle in cm,
z = viscosity of the liquid in poises,
s_p = specific gravity of the particle, and
s_l = specific gravity of the liquid.

Thus, the settling velocity varies directly with the square of the effective particle diameter. Then at any point between the milling faces of the mill, particles of different sizes will tend to move at different linear radial velocities in accordance with equation (16). Furthermore, as a result of these differential velocities, the coarser particles will tend to accumulate adjacent to the rotor and toward the periphery of the mill, while the finer particles will tend to accumulate adjacent to the stator and toward the axis of rotation. The resulting distribution of particle sizes is illustrated in Figure 5. When the combined effects of particle size segregation and fluid velocity profile are considered, one can see that coarser particles will tend to move toward the rotor and then downward toward the periphery until they are disintegrated by fluid shear and attrition, while the finer particles will tend to be displaced inward toward the stator and then upward through the annulus and finally out of the mill.

Although equation (16) has been used as a basis for this discussion, the settling velocity need not conform exactly to this particular expression in order for the mill to work.

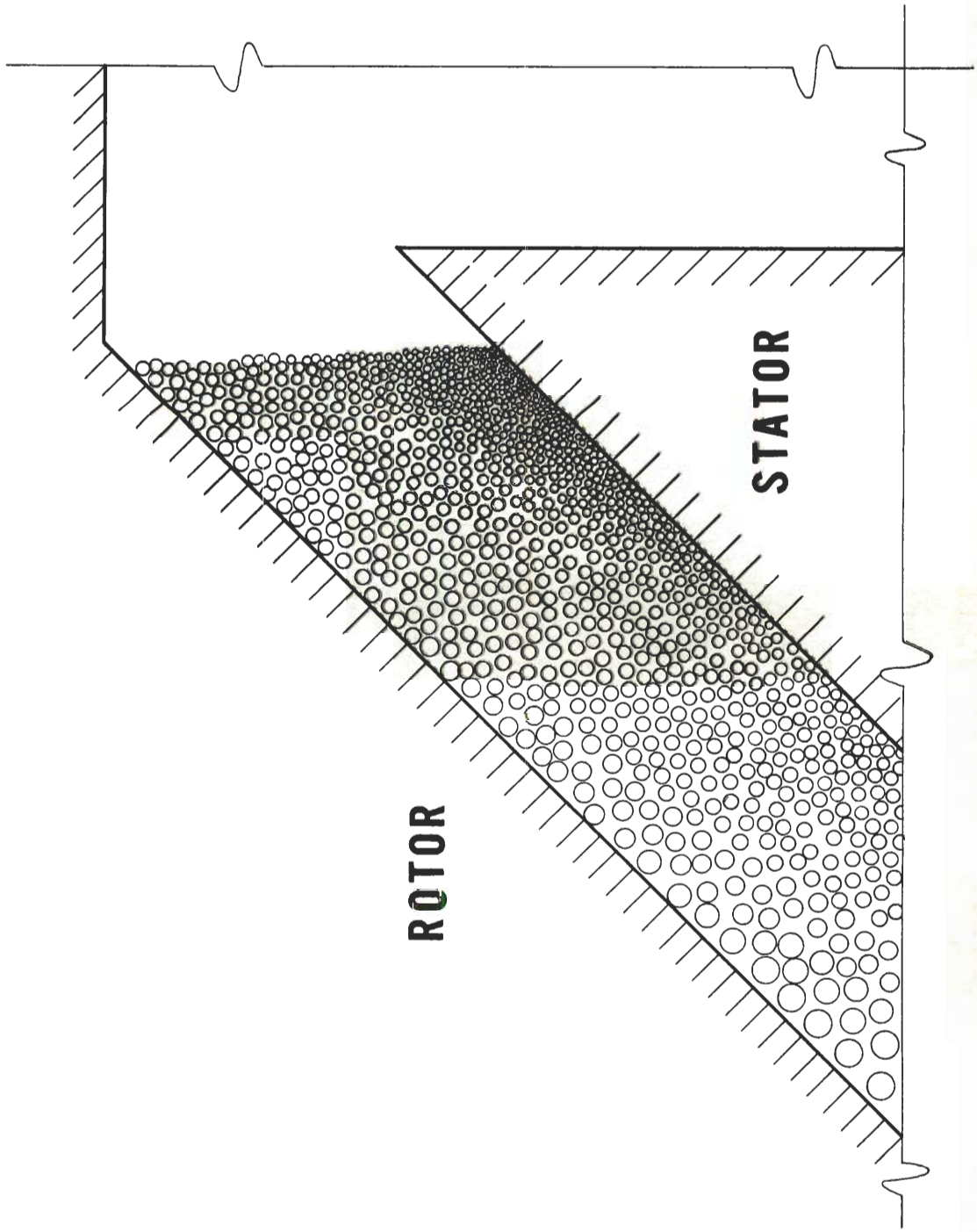

Figure 5. Representation of Particle Distribution.

CHAPTER III

DESIGN AND CONSTRUCTION OF THE MILL

Specific design considerations.--The construction of a prototype of the modified mill was made possible through the cooperation of the Georgia Tech Engineering Experiment Station in making available a Model B-1402 Morehouse Mill and in providing the machine work for the modification parts. Fortunately, the frame of the Morehouse Mill was adaptable to the required modifications; this provided a well-advanced starting point and eliminated many of the mechanical engineering design problems.

At the same time, the use of the Morehouse Mill frame imposed certain limitations on the design variables. However, these limitations were actually helpful in establishing a design since several variables were thereby eliminated. The Morehouse Mill is driven by a 20-hp motor at 3600 rpm and the casing will accommodate a rotor not exceeding 7 inches in diameter. Furthermore, the stator annulus cannot be less than about 2.5 inches in diameter in order to accommodate the drive shaft and rotor sleeve properly. Thus, at the outset two variables were fixed and two others were limited.

The first design variable to be determined was the angle θ. The effect of the magnitude of this angle on the velocity profile of the fluid is given in equation (8) of Chapter II. Consideration of two limiting cases shown in Figure 6 will further elucidate this effect. At an angle of 90°, shown in (a), $\cos \theta = 0$ and the velocity profile is

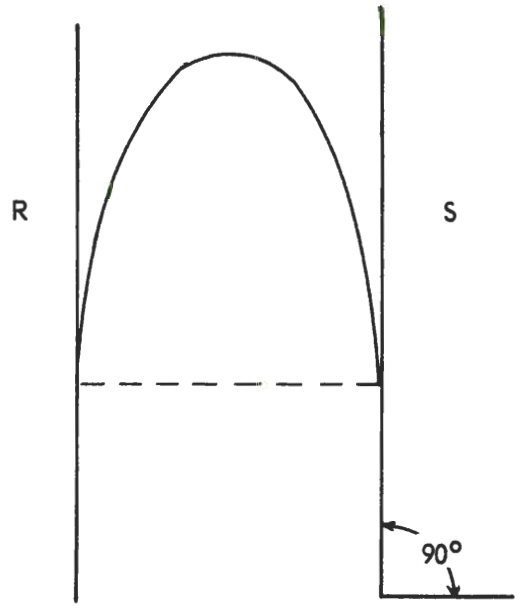

(a)

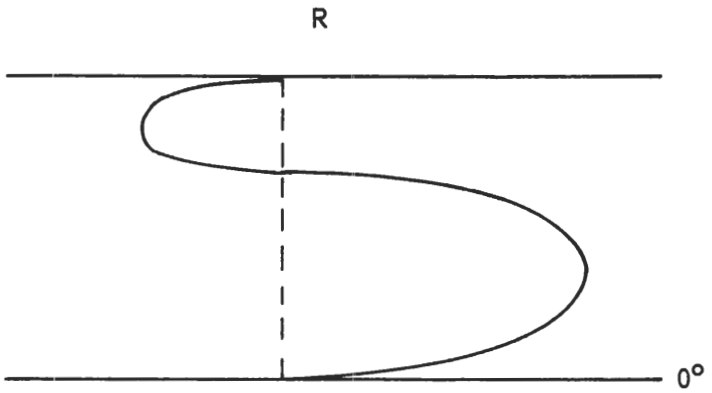

(b)

Figure 6. Velocity Profiles at 90° and 0°.

essentially a simple parabola slightly skewed outward. For a fluid containing suspended solids, coarse particles will achieve maximum segregation from fine particles in the minimum time because they travel the shortest path possible. However, because of the approximately symmetrical velocity distribution, there is no selective retardance of coarse particles in the milling zone and no effective classification will occur with respect to materials discharged. At the other extreme, 0°, shown in (b), $\cos \theta = 1$ and the maximum effect of centrifugal force on the velocity profile is manifested. An actual reversal of the direction of flow may occur adjacent to the rotor. But since centrifugal force does not act to produce segregation of coarse particles toward the rotor, the potential advantages of the unusual velocity distribution to produce internal classification are not exploited.

Obviously the optimum angle, θ, for any slurry or light paste will lie somewhere between the limiting cases. However, since the properties and concentrations of liquid-solid systems that are of interest vary widely, the decision was made to set the angle θ at 45° and, thus, make it a constant for the present study.

The radial dimensions of the milling faces are represented in Figure 2 of Chapter II by the letters a for the peripheral radius and b for the annular radius. Practical limitations of these dimensions have been given. The actual design dimensions were largely dictated by a desire to construct a piece of equipment, the dimensions of which could be changed in accordance with the findings of preliminary experiments. Thus, the dimension a was set at 3.5 inches and the dimension b was set at 1.75 inches.

A more theoretical justification for the specific design was developed in terms of projected mill operation, although again the theory involves assumptions and reservations. From equation (16) of Chapter II, the settling velocity was defined as

$$V_s = \frac{d^2}{18z} (s_p - s_l) r\omega^2.$$

Now obviously

$$V_s = \frac{L}{T} \tag{17}$$

where L is the settling length and T is the settling time. Then if the required settling length for classification is assumed to be one-half the horizontal distance between milling faces, one can write

$$L = \frac{c}{2 \sin \theta} \tag{18}$$

where c is the distance between milling faces. Also the average settling time can be expressed as

$$T = \frac{U}{Q} \tag{19}$$

where U is the total volume in the milling zone and Q is the rate of flow. Also, to a close approximation

$$U = \pi l (a + b)c \tag{20}$$

where l is the slant height of the cone. Finally, substituting equations 17, 18, 19, and 20 in equation (16) yields

$$\frac{d^2(s_p - s_l)}{Qz} = K \qquad (21)$$

where K is a constant that includes r as the mean radius and ω as one-half the angular velocity of the rotor. Upon selection of convenient units for the variables, this expression becomes

$$\frac{d^2(s_p - s_l)}{Qz} = 4.46 \times 10^{-1} \qquad (22)$$

where the units are

d = particle diameter in microns,
s_p = density of solid particles, in pounds per gallon (of solid),
s_l = density of liquid in pounds per gallon,
Q = flow of paste in gallons per hour, and
z = viscosity of paste in centipoises.

Based on equation (22), corresponding values for the variables are given in Table 1.

The figures given in Table 1 are interpreted as merely indicative of the relative classifying effectiveness of the mill under various conditions.

The problem of heat dissipation is another important design consideration. While the mill motor is rated at 20 hp, the power input to the mill that must be dissipated as heat may vary, depending upon the operating conditions. Linseed oil has a specific heat of about 0.44 cal/g/°C. This is about the lowest specific heat that is likely to be encountered. Accordingly

$$0.44 \times T \times q = 1.07 \times 10^4 \times P.$$

Table 1. Theoretical Classification Performance

d (microns)	$s_p - s_l$ (lb/gal)	z (cp)	Q (gal/hr)
10	10	100	22.4
20	10	100	89.7
10	20	100	44.8
20	20	100	179.4
10	10	1000	2.2
20	10	1000	9.0
10	20	1000	4.5
20	20	1000	17.9

where $\underline{T}$ is the temperature rise in degrees centigrade, $\underline{q}$ is the rate of flow in grams per minute, and $\underline{P}$ is the horsepower. The factor 1.07×10^4 is the gram-calorie per minute equivalent of one horsepower. Rearrangement and conversion to convenient units is accomplished as follows:

$$q\left(\frac{g}{min}\right) = Q\left(\frac{gal}{hr}\right) \times 7.8\left(\frac{lb}{gal}\right) \times 454\left(\frac{g}{lb}\right) \times \frac{1}{60}\left(\frac{hr}{min}\right)$$

$$= 59.0\ Q$$

$$TQ = \frac{1.07 \times 10^4}{0.44 \times 59.0} P$$

$$TQ = 414\ P \qquad (23)$$

where

T = temperature rise in degrees centigrade,
Q = rate of flow in gallons per hour, and
P = horsepower input.

In the application of equation (22) the total input of heat is assumed to be retained by the fluid. Actually, some of this heat is dissipated in the water-jacketed mill. Therefore, one may anticipate that the actual temperature rise will be slightly less than that predicted by the equation. As a guide for mill operation, $\underline{T}$ is plotted against $\underline{Q}$ at 5, 10, 15, and 20 horsepower in Figure 7.

Finally, a calculation of the power requirements of the mill under various operating conditions is of interest. The basis for this calculation is equation (1) of Chapter II. With the exception of the viscosity, $\underline{z}$, and the clearance, $\underline{c}$, all of the factors of this equation may be combined into a constant, $\underline{K}$. Thus, the expression becomes

$$P = K \frac{z}{c}.$$

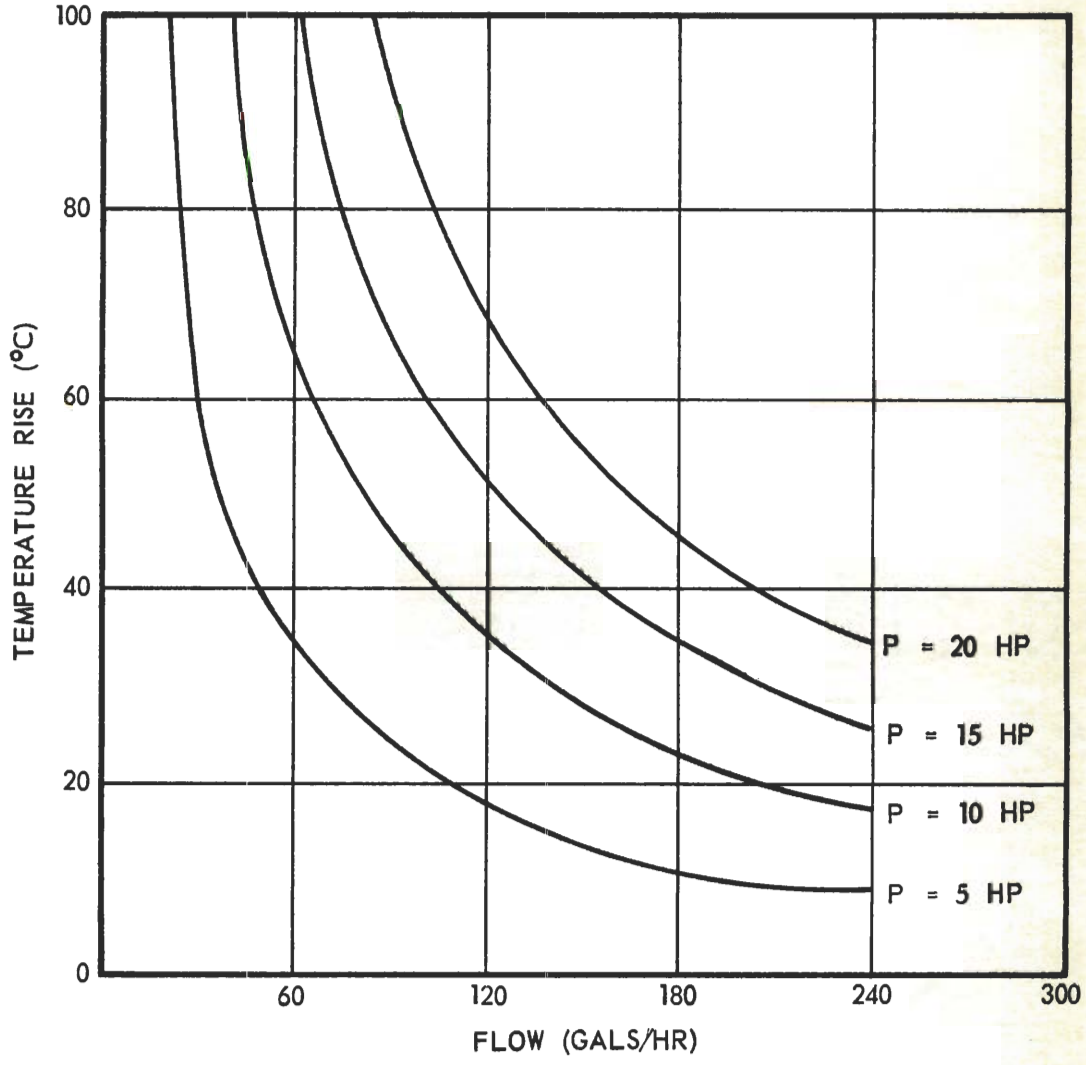

Figure 7. Theoretical Temperature Rise as a Function of Flow Rate.

When K is evaluated for the desired units, the specific equation may be given as

$$z = 1.03 \times 10^{3} Pc \qquad (24)$$

where

z = viscosity in centipoises,
c = clearance in inches, and
P = horsepower input.

As a further guide to mill operation, z is plotted against c for 5, 10, 15, and 20 horsepower in Figure 8. Since equation (24) deals only with the power consumption in the milling zone, actual horsepower requirements for the mill should be somewhat higher.

In a later chapter, the design considerations presented here will be subjected to a re-evaluation in the light of experimental data.

Mill assembly and instrumentation.--The modification of the Model B-1402 Morehouse Mill was accomplished without any machine work on the existing mill. The rotor and head assembly were simply removed and replaced with the required parts for the new design. A detailed mill assembly drawing of these parts is shown in Figure 9. The inner casing was fabricated from 8-in. diameter steel tubing with the flanges welded on. The upper flange is bolted securely to the studs on the rim of the mill. The stator, which was turned from solid steel stock, is bolted onto the lower flange of the casing. The head of the mill was fabricated from an 8-in. steel welding cap. The cap was flanged to match the casing, and a hole was cut into the crown to accommodate a 2-1/2-in. pipe nipple. The construction of the rotor assembly required the most machine work. First,

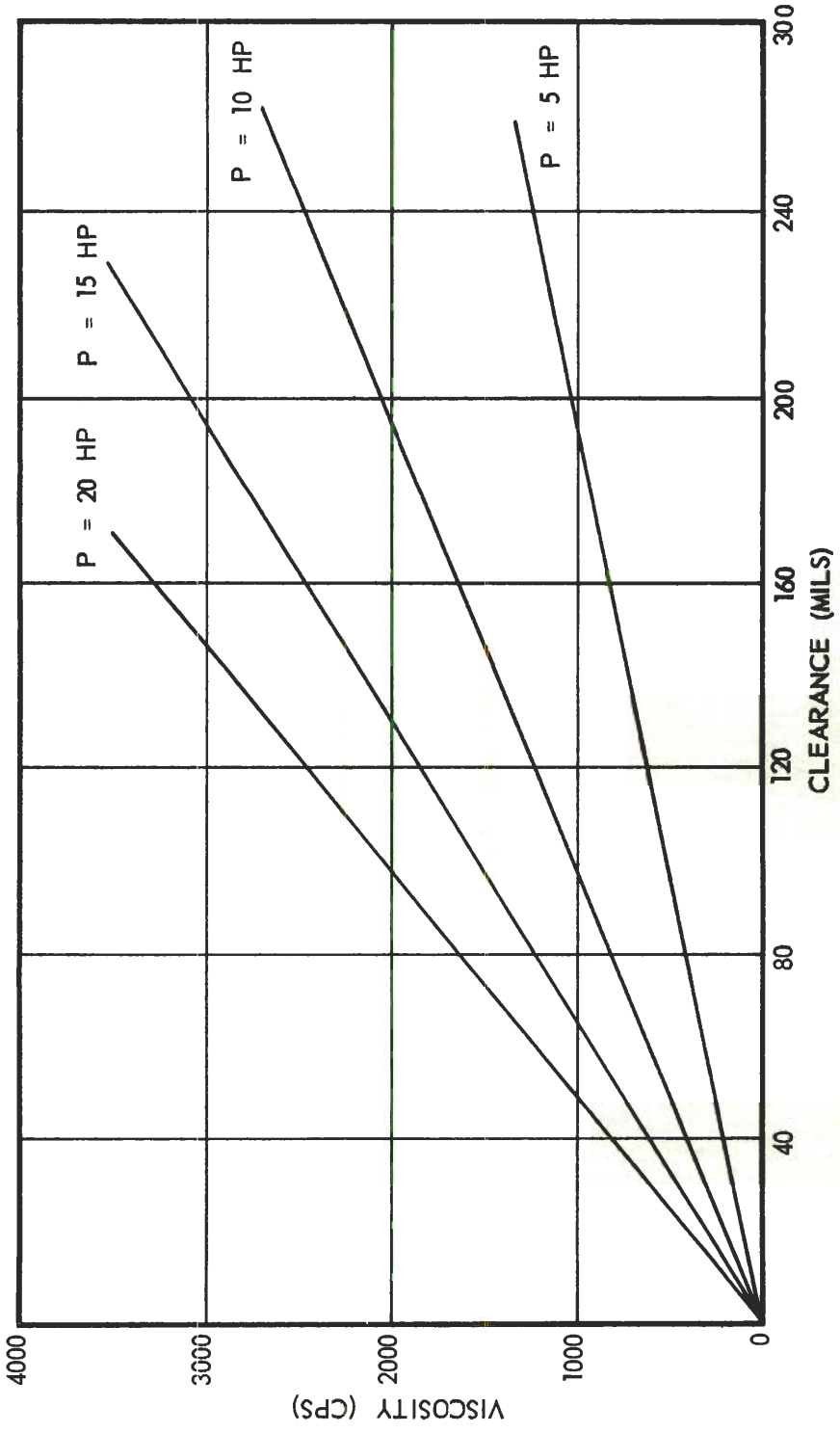

Figure 8. Theoretical Power Requirements Under Various Operating Conditions.

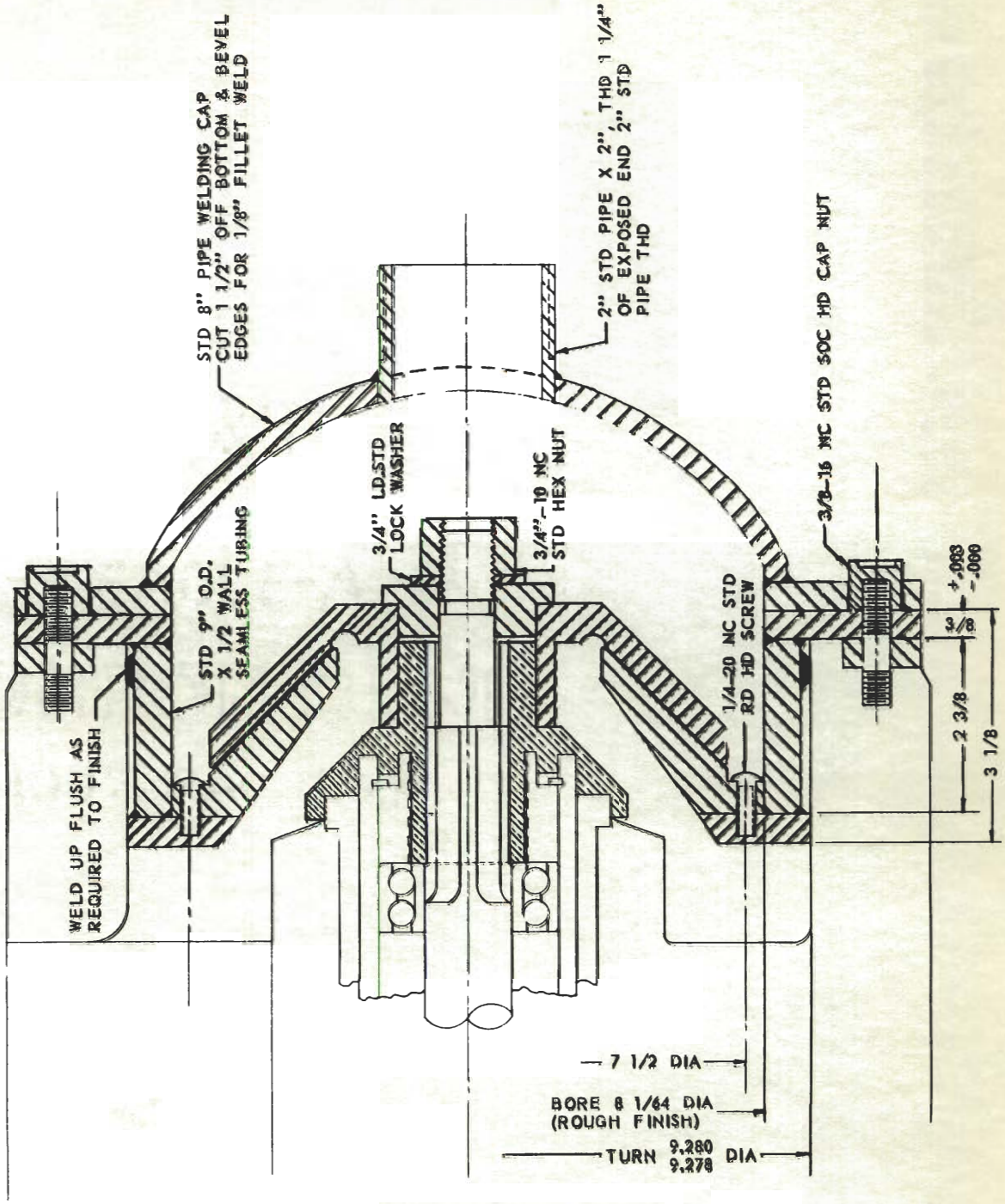

Figure 9. Detailed Mill Assembly.

it was necessary to make a rather complex brass bushing to fit over the splined drive shaft and into a ring labyrinth seal at the bottom. The rotor, turned from steel stock, is keyed to the bushing. A lengthy lapping operation was necessary to bring the rotor and stator into satisfactory registration as matched cones. These are the primary parts of the mill.

The inlet atop the head of the mill is connected to a five-gallon reservoir through a No. 2 Goulds rotary pump. The pump is driven by a 1/2-hp motor through a Vickers variable-speed drive with V-belt couplings. These features as well as the instrumentation are illustrated in the photograph of Figure 10.

Static fluid pressure in the head cavity is measured by means of a pressure gage tapped into the head on the front. Wattmeter instrumentation for measuring power consumption is mounted on a table to the left of the mill. These were the only permanently mounted instruments on the equipment.

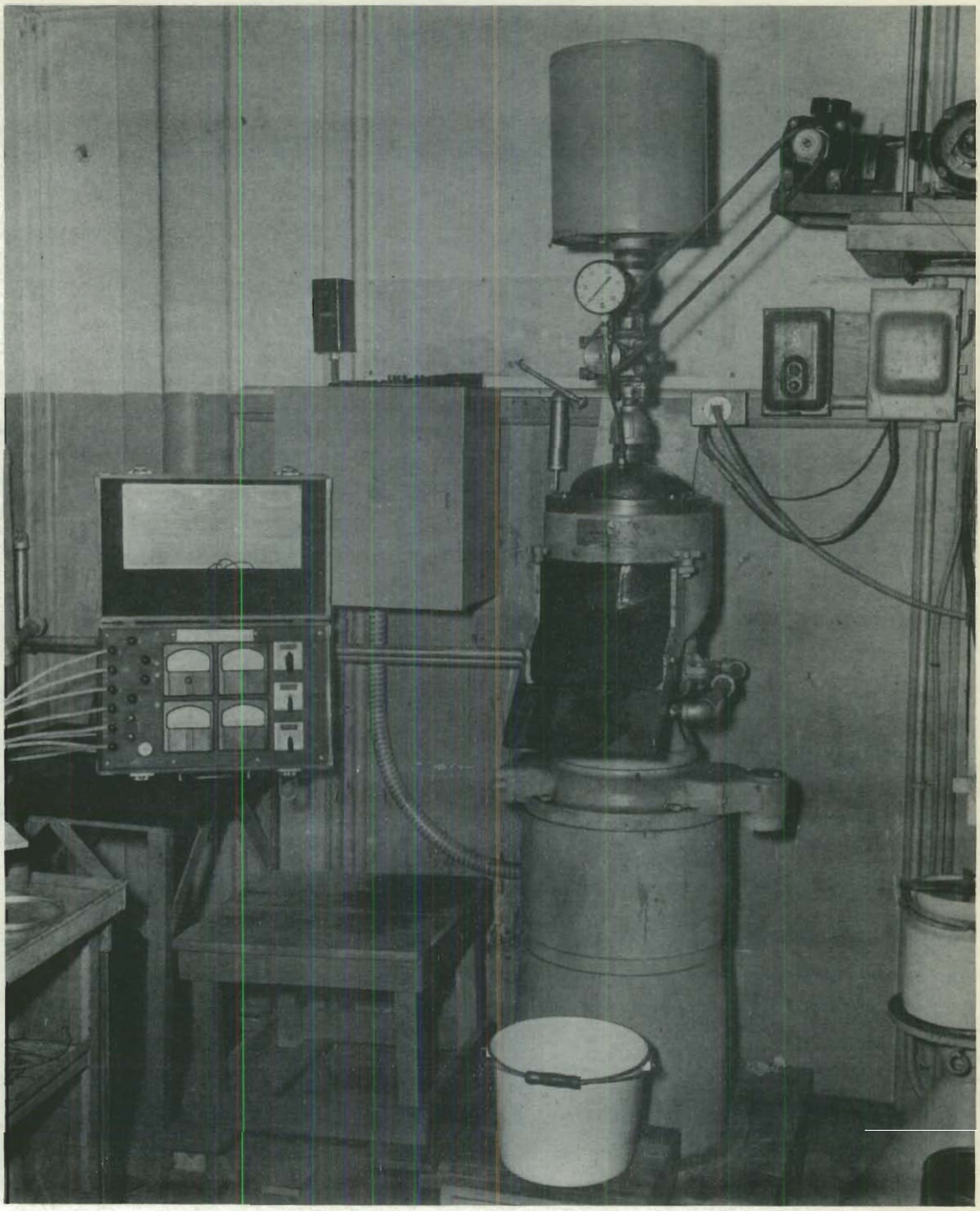

Figure 10. Experimental Equipment.

CHAPTER IV

EXPERIMENTAL WORK

Studies of mill performance were undertaken to define the fluid flow characteristics of the equipment and to evaluate the practical effectiveness of the mill in producing pigment dispersions.

Composition of Liquid Systems

Altogether seven types of liquid systems were studied, namely:

1. water,
2. mineral oil,
3. mineral oil - 25% clay (Paste No. 1),
4. mineral oil - 50% clay (Paste No. 2),
5. white enamel, (Paste No. 3),
6. house paint paste (Paste No. 4), and
7. aqueous dispersion (Paste No. 5).

The mineral oil was obtained from the Standard Oil Company of Kentucky, 1080 Bankhead Avenue, Atlanta, Georgia. It has a viscosity of 250 SAE and is identified as Standard Gear Oil No. 250. Velvacast brand clay produced by the Georgia Kaolin Company, Dry Branch, Georgia, was used. The paint raw materials used in Paste Nos. 3, 4, and 5, were obtained from regular suppliers to the paint industry, and as such, are typical of the ingredients used in commercial products. Formulation details for each of the pastes are given in Appendix B.

The first four of the liquid systems were used only for studying fluid flow. The last three systems, which were representative of commercial paint formulations, were used in part for studying fluid flow, but primarily for evaluating the pigment-dispersion capacities of the mill.

Milling Procedure

Preparation.--The first two systems comprising water alone and mineral oil alone required no preparation for milling. All of the other systems required premixing prior to milling. The ingredients for each paste were combined in a large bucket and mixed manually with a spatula until a smooth paste was obtained.

Flow experiments.--During experimental runs, the following quantities were noted and recorded:

1. rotor clearance,
2. pressure,
3. flow rate,
4. temperature, and
5. power consumption.

As a preliminary step in the study of oil-clay pastes, these mixtures were run through the mill several times to effect a stable dispersion for flow experiments. About three gallons of liquid were charged into the equipment for each study, and this liquid was used repeatedly for multiple runs. Usually, each recorded run was made twice; during the first run, pressure was set and the temperature and power consumption were recorded, and during the second run, the pressure was carefully maintained while the flow rate was determined.

The pressure- and power-measuring devices were described in Chapter III. Rotor clearance was set by means of the handwheel adjustment on the mill. Previous calibration of the handwheel indicated that the rotor could be positioned in this manner with an accuracy of better than one mil in 100 mils of adjustment. Temperature measurement was made with

a mercury thermometer placed directly under the exit annulus. Flow rates were determined by timing the collection of about two gallons of liquid with a stopwatch. The actual quantity collected was determined accurately by weighing.

A serious limitation of the experimental work was the inability of the pump to produce sufficiently high pressures. For this reason, it was usually not feasible to study more than two pressure levels for any given rotor clearance. Likewise, this also limited the minimum rotor clearance that could be studied.

Dispersion experiments.--Since the required raw materials for the pigment-vehicle pastes used in the dispersion studies were relatively expensive, particular attention was directed toward the execution of satisfactory experimental procedures that would minimize the consumption of the paste materials. An effort was made to utilize the data obtained from the previous flow experiments in setting the operating conditions for each dispersion experiment. The flow data obtained in each dispersion experiment were intended primarily to define the operating conditions for that particular run rather than for use in flow correlations.

Between two and three gallons of each type of paint paste were prepared for this work. Only a portion of the total quantity of each paste could be used for a single run because a study of the dispersion effects of a single pass of the paste through the mill under various operating conditions was desired. The necessary subdivision was accomplished by halting the mill at intervals, changing the rotor setting, collecting the fraction of milled product, and resuming the milling operation under

new conditions. In the case of Paste No. 3, a second pass of this material through the mill was run to determine if this procedure would enhance the degree of dispersion.

Data identical to that obtained with the flow experiments were obtained with the dispersion studies; but, in addition, it was necessary to measure the degree of dispersion for each run. The procedure for this determination is included among the physical tests described in the next section.

Physical Tests

To characterize the liquids and pastes for the purposes of this study, viscosities and densities were measured over a range of temperatures and for dispersion experiments fineness of grind or pigment dispersion was measured after each run.

Viscosity determinations.--A Brookfield Viscometer Model LVF was used for the measurement of viscosities over a temperature range of 30° to 170° C. All measurements were made at the maximum spindle speed of 60 rpm. In determining viscosity-temperature relations over the indicated temperature range, it was usually necessary to use all of the four spindles provided with the instrument in order to accommodate the large viscosity range.

Density determinations.--Densities were determined by filling a 100-ml volumetric flask to the mark with the liquid at the required temperature and weighing the contents.

Degree of dispersion.--The Hegman Gage, which is usually described as the fineness-of-grind gage, was used in measuring dispersion. This type of gage has been generally accepted by the paint industry as a standard means of evaluating dispersions. A detailed discussion of the application of this gage has been presented in a paper by Baker and Vozzella (17). The relations of grind gage results to particle-size distribution, gloss, and hiding power of paint films have been established.

The grind gage consists of a rectangular steel block, one face of which is polished flat. Into the polished face, a shallow channel about 1/2 inch wide and 6 inches long is milled. This channel is cut at a slight angle to the face of the block so that the depth of the channel varies from zero at one end to five mils at the opposite end. A scale graduated linearly from zero (at five mils) to eight (at zero mils) is engraved alongside the channel. This arbitrary scale is known as the North Standards Scale (NSS).

To make a determination, a small amount of paste is thinned with the proper amount of thinner to produce a consistency representative of the final paint. Several large drops of this material are placed in the deep end of the gage channel. A scraper blade is then swept slowly over the block from the deep to the shallow end of the channel. This produces a wedge of paint in the channel that varies from five to zero mils in depth. When this paint wedge is inspected at an angle of about 15 degrees with the surface, protrusions of pigment agglomerates through the paint film may be observed at various points depending on the size of the agglomerates. The "grind" on the North Standards Scale is taken as the point

where the agglomerates first appear in appreciable numbers. Obviously, this is not a precise method for determining particle size distribution; it is sufficient however, for evaluating the degree of dispersion of paint products and the dispersion performance of milling equipment.

CHAPTER V

EXPERIMENTAL RESULTS

Preliminary data.--Viscosity and density data on water were obtained from the International Critical Tables (18). The viscosities of other liquids were determined experimentally, and the densities were either obtained experimentally or calculated from experimental data on the paste constituents. Detailed plots of viscosity and density as a function of temperature for mineral oil, Paste No. 1, and Paste No. 2 are given in Appendix B, Figures 11, 12, and 13. Viscosity and density data for all of the experimental liquids determined at the average milling temperature of each liquid are included in Table 3.

Power data.--Power consumption was measured in a total of 18 runs; nine runs were made with mineral oil and nine runs were made with Paste No. 1. In each case, within the limits of the experiments, power consumption was constant and independent of rotor clearance or pressure drop. The results are summarized below:

Table 2. Power Consumption

Fluid	Net Power Input (hp)
Mineral Oil	2.01
Paste No. 1	2.68

Table 3. Experimental Flow and Dispersion Data

(Values of T, z, and s are averages for calculation purposes)

p(psig)	C(mils)	Q(gal/hr)	p(psig)	c(mils)	Q(gal/hr)
Water			**Paste No. 1**		
T = 70° C			T = 130° C		
z = 0.41 cps			z = 30.0 cps		
s = 0.98			s = 1.015		
8.0	48.8	0.0†	10.0	70.7	35.0
8.0	56.5	16.2	11.0	70.7	130.6
8.5	56.5	41.6	13.0	49.5	28.6
9.0	48.8	27.0	14.0	35.4	18.0
10.0	27.6	0.0	14.0	49.5	95.4
			16.0	21.2	19.3
			17.0	35.4	71.4
			18.0	14.1	17.9
			19.0	21.2	41.9
Mineral Oil			**Paste No. 2**		
T = 140° C			T = 170° C		
z = 15.0 cps			z = 50.0 cps		
s = 0.865			s = 1.23		
5.0	70.7	18.4	8.0	70.7	0.0
9.0	56.5	0.0	10.0	70.7	18.0
10.0	42.4	29.2	12.0	70.7	63.8
11.0	35.4	0.0	14.0	49.5	5.1
12.0	28.3	0.0	16.0	49.5	33.6
12.0	31.8	0.0	17.0	42.4	0.0
13.0	24.7	0.0	18.0	35.4	0.0
14.0	21.2	43.5	19.0	28.3	13.1
15.0	17.7	38.3	20.0	21.2	17.4
			20.0	14.1	3.8
			22.0	28.3	63.6
			24.0	21.2	46.0
			24.0	14.1	22.5

†Zero flow values indicate impending or immeasurably small flow.

Table 3. Experimental Flow and Dispersion Data
(Values of T, z, and s are averages for calculation purposes)

p(psig)	c(mils)	Q(gal/hr)	No. of Passes	Grind(N.S.S.)
Paste No. 3				
T = 130° C z = 370 cps s = 1.48				
25.0	14.1	8.5	1	0
30.0	10.6	12.0	1	0
40.0	10.6	21.2	1	0
40.0	7.1	19.8	2	1
Paste No. 4				
T = 120° C z = 1080 cps s = 1.47				
30.0	7.1	11.9	1	3
40.0	3.5	5.5	1	3
Paste No. 5				
T = 64° C z = 1000 s = 1.33				
10.0	46.0	0.0	1	3
10.0	49.4	2.6	1	3

In determining power consumption, the power was first measured while the mill was running free with no liquid in the cavity. The power required under this condition was assumed to represent all frictional losses not assignable to the liquid. The "Net Power Input" was then obtained by subtracting the "free-running power" from the total power reading on the wattmeter.

Flow and dispersion data.--Information was collected from 44 experimental runs in this work. Experiments with water, mineral oil, Paste No. 1, and Paste No. 2 involved 36 runs were directed at a study of fluid flow. The final eight runs with Pastes No. 3, No. 4, and No. 5 were intended primarily for the study of dispersion, but additional information was also gained on fluid flow. The results are given in Table 3.

CHAPTER VI

DISCUSSION OF RESULTS

Pressure drop correlations.--A theoretical approximation for pressure drop was given in Chapter II, equation (14). The first term of this equation obviously represents the pressure drop resulting from the centrifugal pumping effect, while the second term represents the frictional pressure drop. For the experimental flow conditions, both of these terms are positive since Q will be taken as positive in the centripetal direction. When numerical values for constants and conversion factors are substituted in the equation, the expression becomes

$$p = (4.6\ s + 0.00082\ sc) + 267.0 \frac{zQ}{c^3} \qquad (25)$$

where

p = pressure in pounds/in^2,
s = density in grams/ml or specific gravity,
z = viscosity in centipoises,
Q = flow in gal/hr, and
c = rotor clearance in mils (0.001 inch).

When experimentally measured values of the variables are substituted in equation (25), the calculated pressure drop is found to depart markedly from experimental values. The theoretical equation does not correlate the variables. Nevertheless, an equation of this general form could be useful for an empirical correlation. Thus, an equation of the form

$$p = p_c - p_f \tag{26}$$

is proposed, where p_c and p_f represent the centrifugal and flow pressure drops respectively. It follows that when

$$Q = 0,\ p_f = 0$$

whereupon

$$p = p_c,$$

and therefore, with sufficient experimental data, p_c and p_f may be evaluated.

From limited experimental data, at given c values, when Q versus p is extrapolated to $Q = 0$, the value of p_c is obtained. This procedure has been applied to the data on Pastes No. 1 and No. 2 by using straight-line extrapolations based on two experimental points. The resulting plots are shown in Figures 14 and 15 respectively. The straight line extrapolation is justified, first, because equation (25) suggests such a relationship; second, because one of each pair of points has a small Q value and therefore the extrapolation is short; and finally, because experimental p values at zero flow are in fair agreement with the extrapolations. These latter points (zero flow) were not used for calculations because they were not as reproducible as points at finite flow rates. The relation of values for pressure at zero flow to rotor clearance is shown in Figure 16.

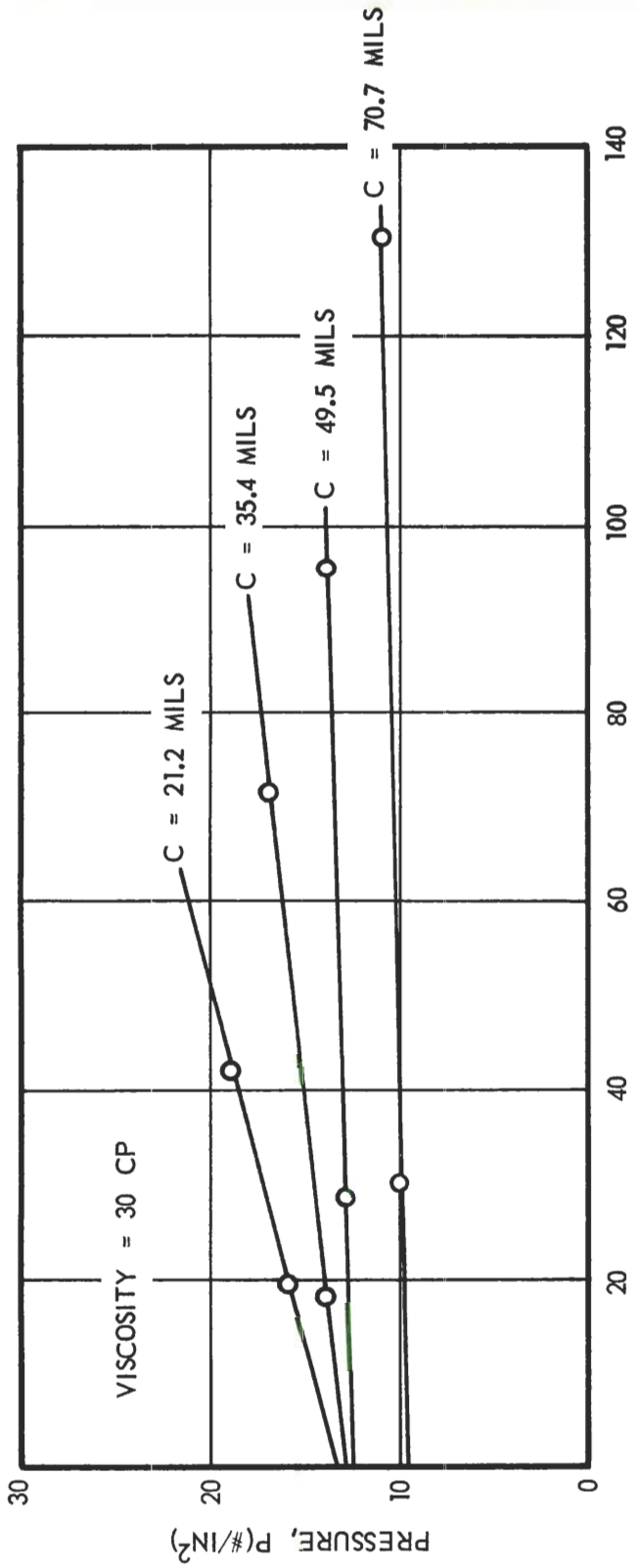

Figure 14. Flow Versus Pressure for Paste #1.

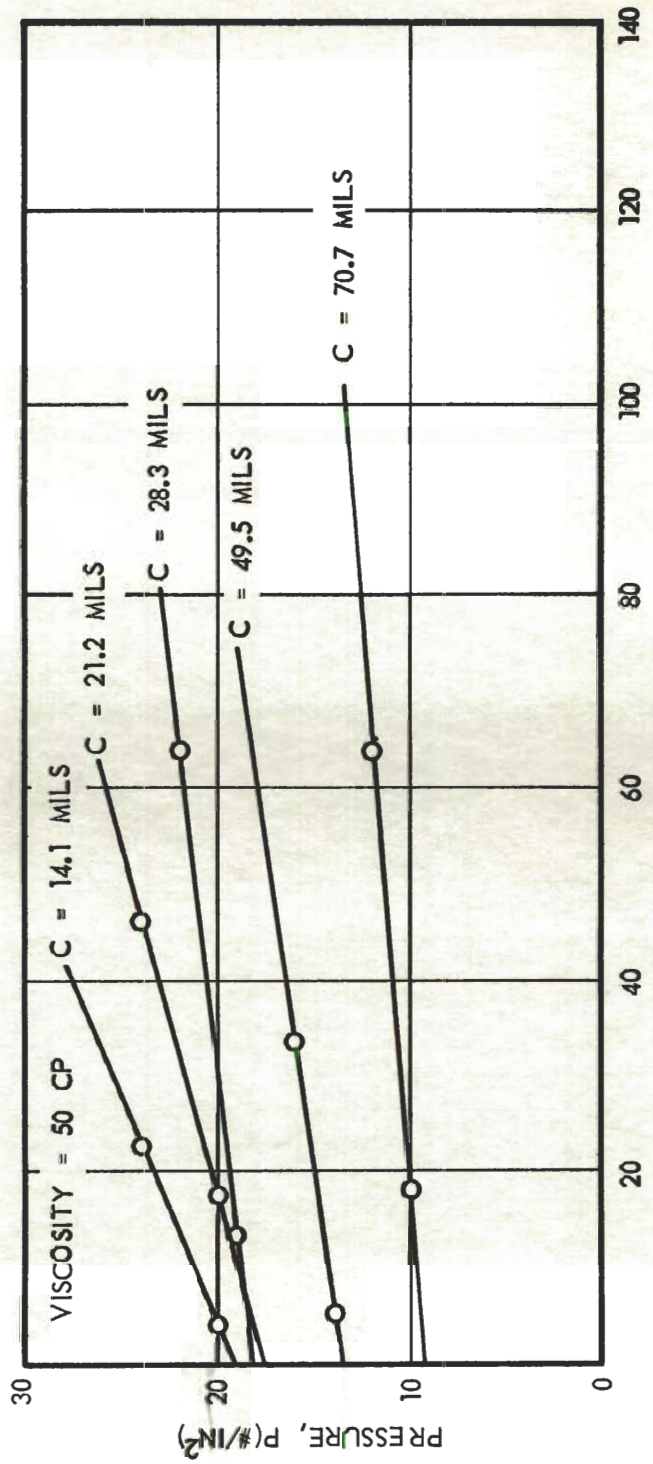

Figure 15. Flow Versus Pressure for Paste #2.

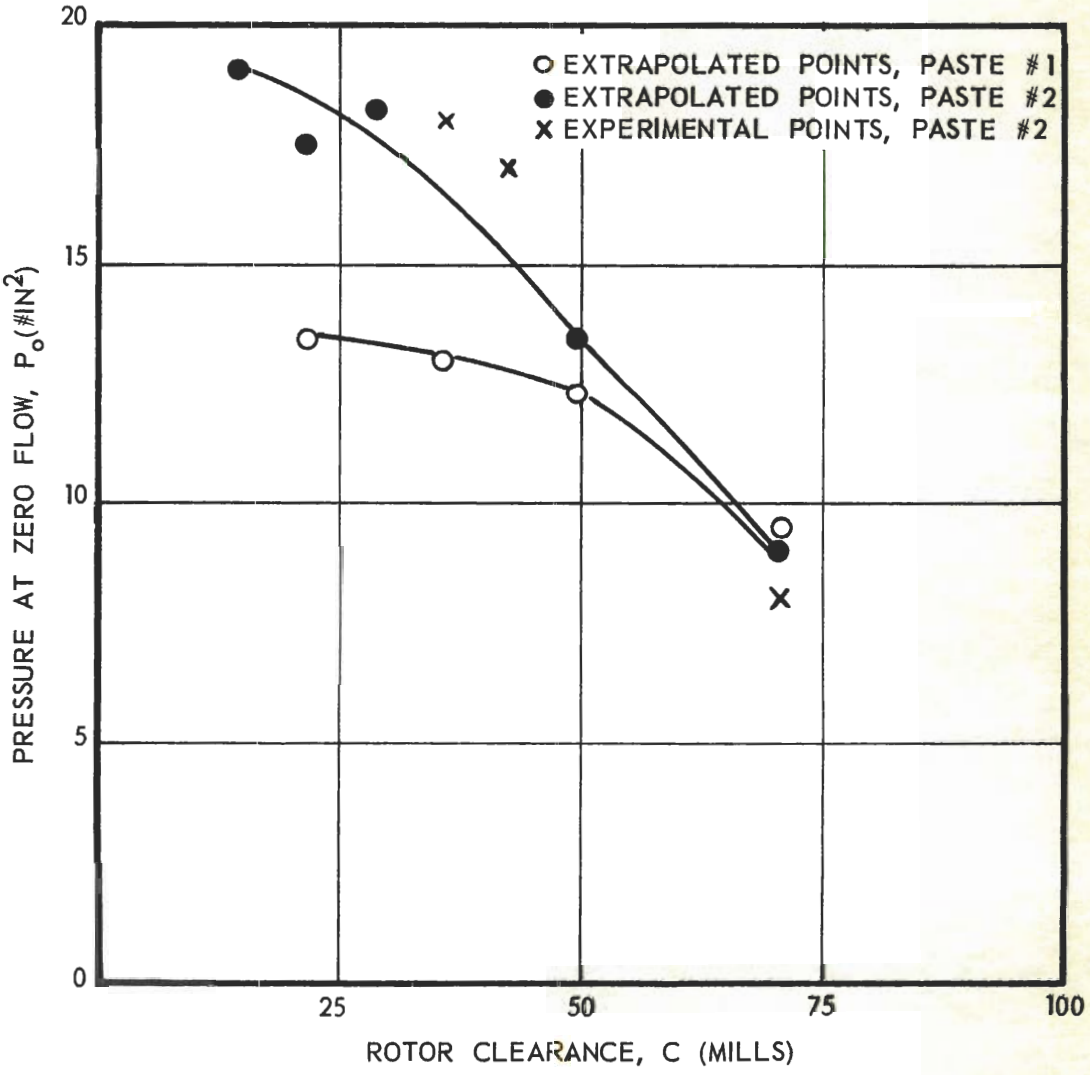

Figure 16. Pressures at Zero Flow as a Function of Rotor Clearance.

After values of p_c and p_f were calculated, an expression was desired for each of these in terms of an empirical constant and a function of the operating variables. Equation (25) was used as a guide and after much trial and error work, the following expressions were evolved:

$$p_c = \frac{K_c}{c^{0.5}}, \quad p_f = \frac{K_f z Q}{c^2},$$

$$P = \frac{K_c}{c^{0.5}} + \frac{K_f z Q}{c^2}. \tag{27}$$

One will note that the "centrifugal pressure term" departs markedly from the theoretical form.

Tabulations of the calculated data and constants are given in Table 4. Note that for Paste No. 1, reasonably constant values are obtained for K_c and for K_f. For Paste No. 2, K_c is fairly constant but K_f gives two groups of values. Observe, however, that within each of these groups, the values of K_f are reasonably constant. This observation suggests the possible occurrence of a flow transition with Paste No. 2.

To summarize the foregoing discussions, experimental points together with the correlation of equation (27) are plotted for Pastes No. 1 and No. 2 in Figures 17 and 18 respectively.

The correlations based on Paste No. 1 and No. 2 are applicable to these materials only, and the presentation on coordinates of $\underline{p}$ and $\underline{c}$ necessarily involves $\underline{Q}$ as a parameter. Therefore, an approach to a more generalized correlation is desirable. Equation (27) may be taken

Table 4. Tabulation for Correlation

p (psig)	c (mils)	Q (gals/hr)	p_c (psi)	p_f (psi)	K_c ($p_c c^{0.5}$)	K_f $\left(\frac{p_f c^2}{ZQ}\right)$
			Paste No. 1			
			T = 130° C z = 30.0 cps s = 1.015			
10	70.7	35.0	9.5	0.5	79.0	2.39
11	70.7	130.6	9.5	1.5	79.0	1.91
13	49.5	28.6	12.5	0.5	87.5	1.43
14	35.4	18.0	13.0	1.0	78.0	2.32
14	49.5	95.4	12.5	1.5	87.5	1.28
16	21.2	19.3	13.5	2.5	62.0	1.94
17	35.4	71.4	13.0	4.0	78.0	2.32
18	14.1	17.9	--	-	--	--
19	21.2	41.9	13.5	5.5	62.0	1.97
			Averages		76.6	1.94
			Paste No. 2			
			T = 170° C z = 50.0 cps s = 1.23			
8	70.7	0.0	--	-	--	--
10	70.7	18.0	9.0	1.0	75.6	5.56
12	70.7	63.8	9.0	3.0	75.6	4.71
14	49.5	5.1	13.5	0.5	94.5	4.77
16	49.5	33.6	13.5	2.5	94.5	3.65
			Averages			4.67
17	42.4	0.0	--	-	--	--
18	35.4	0.0	--	-	--	--
19	28.3	13.1	18.2	0.8	96.5	0.98
20	21.2	17.4	17.5	2.5	80.5	1.30
20	14.1	3.8	19.0	1.0	72.3	1.05
22	28.3	63.6	18.2	3.8	96.5	0.96
24	21.2	46.0	17.5	6.5	80.5	1.28
24	14.1	22.5	19.0	6.0	72.3	1.07
			Averages		83.9	1.11

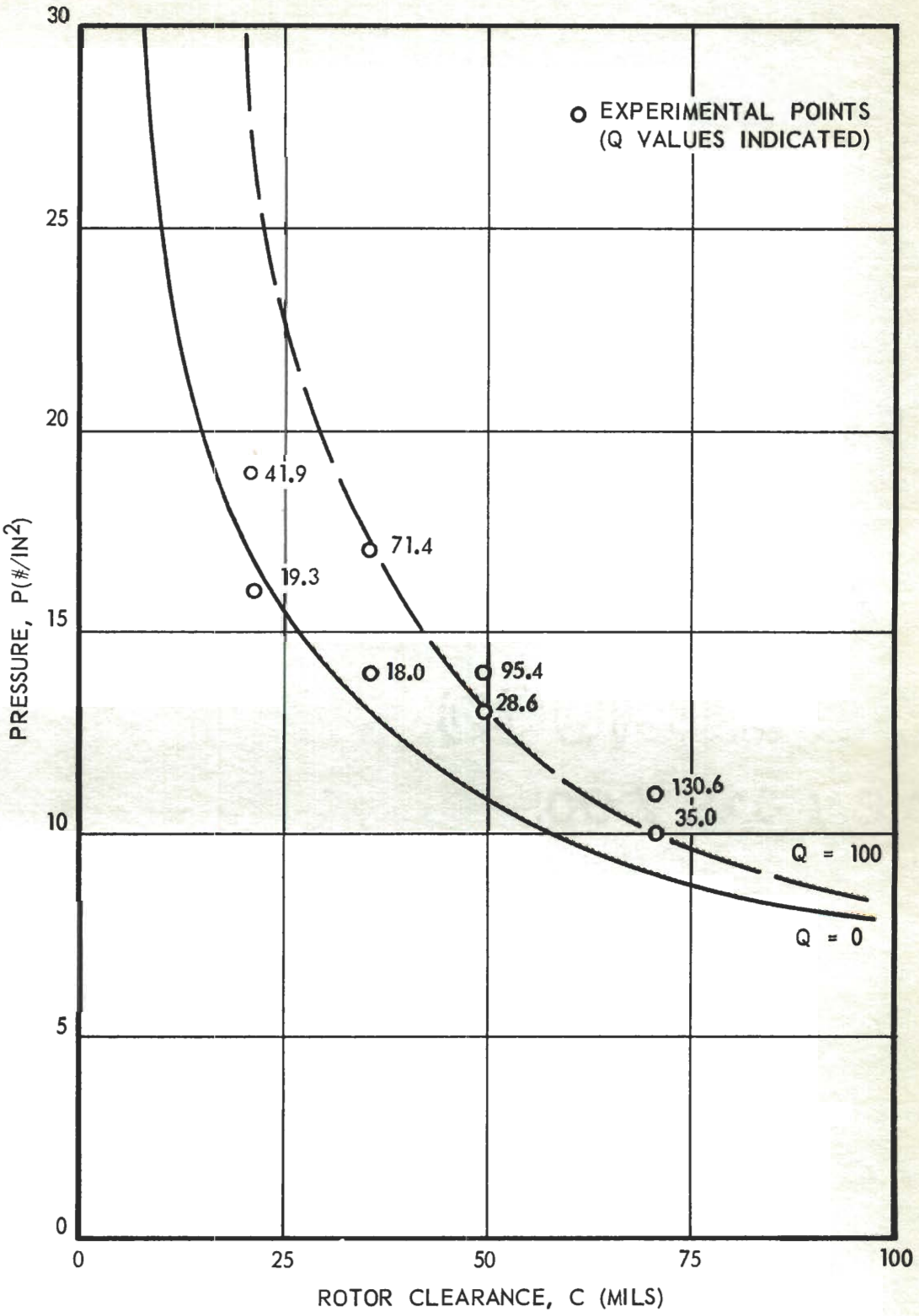

Figure 17. Pressure-Clearance Correlation for Paste #1.

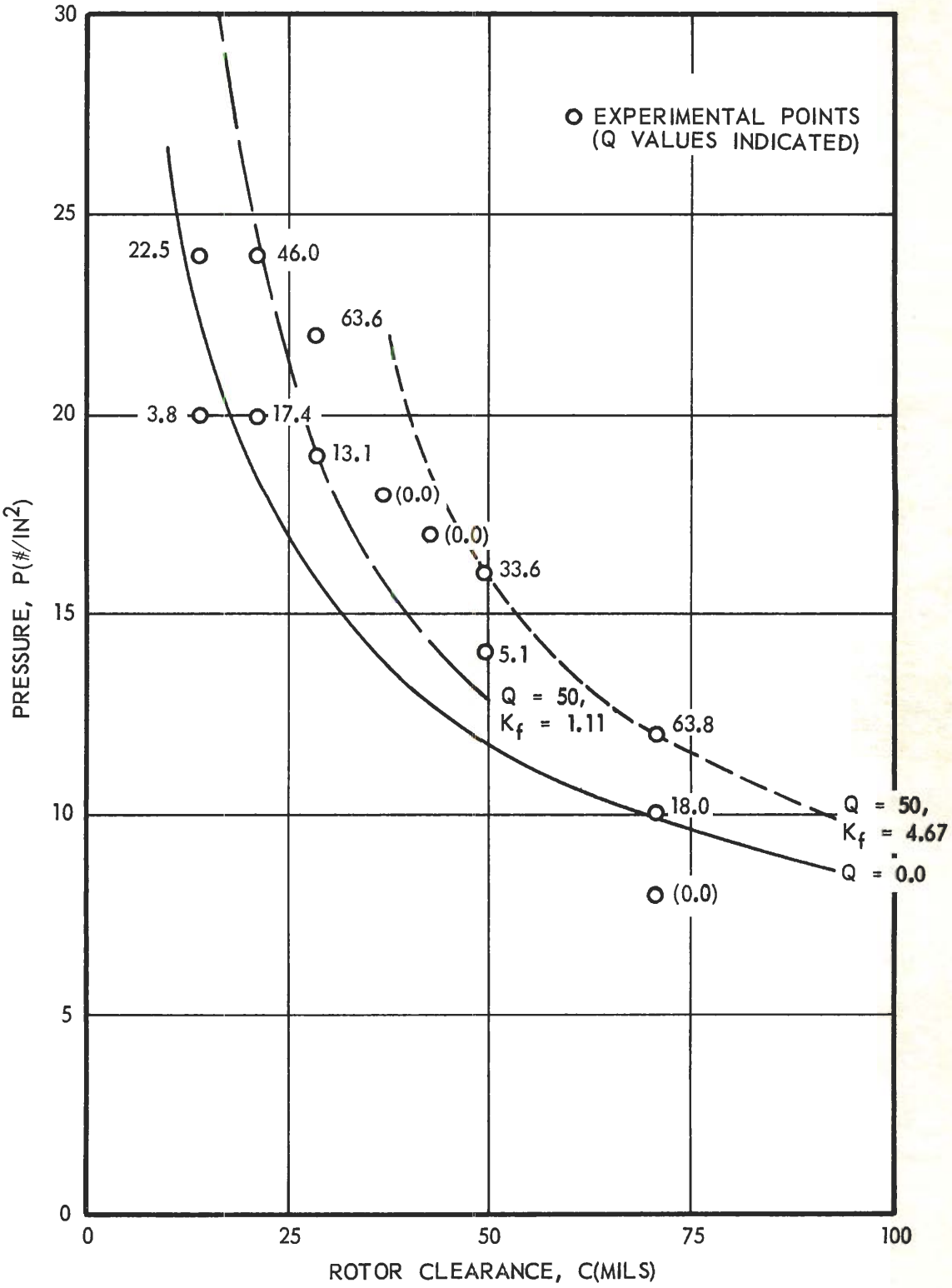

Figure 18. Pressure-Clearance Correlation for Paste #2.

as the basis for this work; but since density, s, becomes a variable in the generalized case it is first necessary to separate this factor from K_c. Accordingly let

$$K_c = K'_c s$$

and

$$p = \frac{K'_c s}{c^{0.5}} - \frac{K_f z Q}{c^2}. \qquad (28)$$

When equation (28) is multiplied by $\frac{c^{0.5}}{s}$ one obtains

$$\frac{p c^{0.5}}{s} = K'_c - \frac{K_f z Q}{c^{1.5} s}. \qquad (29)$$

Thus, if $\frac{p c^{0.5}}{s}$ is plotted against $\frac{zQ}{c^{1.5} s}$, a straight line should be obtained with a slope of K_f and an intercept of K'_c. Data for this correlation are presented in Table 5 for all the experimental materials except Paste No. 5. The runs with Paste No. 5 are not believed to represent adequate operational stability for flow correlation. When the calculated data are plotted, a wide scattering of points is observed as shown in Figure 19. Equation (29) does not correlate the data. This lack of a correlation can be at least partly explained by evidence that K_f is not necessarily a single-valued constant even for a single liquid. This was demonstrated in the previous individual treatment of Paste No. 2. More fundamentally, however, serious limitations of equation (28) must be

Table 5. Data for Generalized Correlation

p	c	$\frac{pc^{0.5}}{s}$	$\frac{zQ}{c^{1.5}s}$	p	c	$\frac{pc^{0.5}}{s}$	$\frac{zQ}{c^{1.5}s}$
Water				Paste No. 2			
8.0	48.8	57.0	0.0	8.0	70.7	54.6	0.0
8.0	56.5	61.0	0.037	10.0	70.7	68.3	1.26
8.5	56.5	65.0	0.103	12.0	70.7	82.2	4.32
9.0	48.8	64.0	0.132	14.0	49.5	79.6	0.61
10.0	27.2	53.0	0.0	16.0	49.5	91.2	3.90
				17.0	42.4	91.2	0.0
Mineral Oil				18.0	35.4	88.0	0.0
				19.0	28.3	81.8	3.56
5.0	70.7	49.0	0.53	20.0	21.2	74.8	7.25
9.0	56.5	78.0	0.0	20.0	14.1	61.8	0.29
10.0	42.4	76.0	1.82	22.0	28.3	95.0	17.20
11.0	35.4	76.0	0.0	24.0	21.2	89.6	19.05
12.0	28.3	78.0	0.0	24.0	14.1	74.2	17.25
12.0	31.8	78.0	0.0				
13.0	24.7	75.0	0.0	Paste No. 3			
14.0	21.2	74.0	7.70				
15.0	17.7	73.0	9.00	25.0	14.1	63.5	40.0
				30.0	14.1	66.1	87.0
Paste No. 1				40.0	10.6	88.0	154.0
				40.0	7.1	71.5	260.0
10.0	70.7	82.7	1.75				
11.0	70.7	91.2	1.18	Paste No. 4			
13.0	49.5	89.6	2.38				
14.0	35.4	82.8	2.52	30.0	7.1	54.5	461.0
14.0	49.5	96.5	8.05	40.0	3.5	78.3	625.0
16.0	21.2	72.5	5.80				
17.0	35.4	100.5	10.06				
18.0	14.1	67.4	10.00				
19.0	21.2	86.0	12.67				

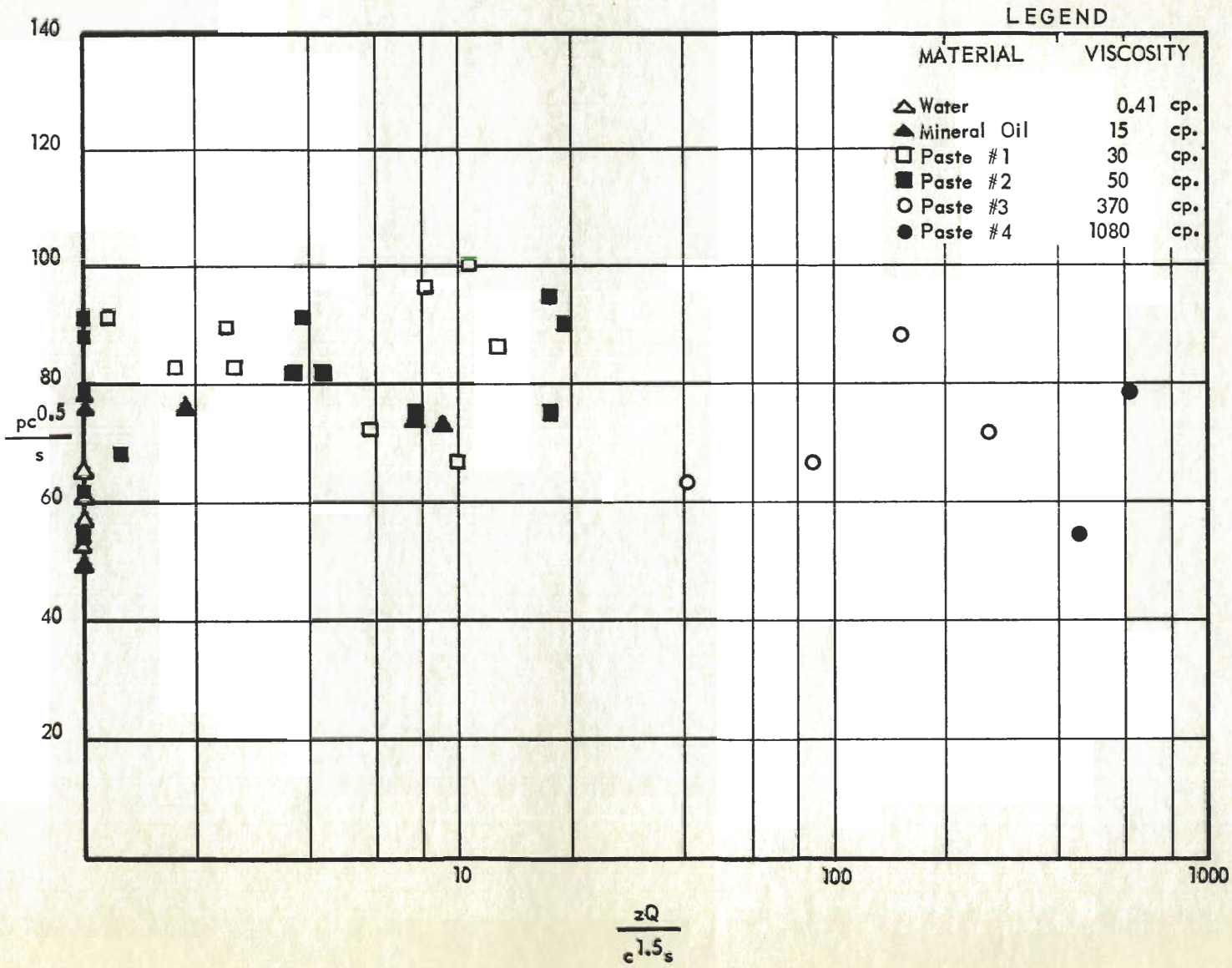

Figure 19. Plot of Generalized Correlation.

recognized. Briefly, this equation is a theoretical approximation, empirically modified. Of particular significance is the fact that the theoretical derivation is based on an assumption of viscous flow. Thus, correlation in the turbulent region should not be expected.

Additional evidence supports the hypothesis of turbulent flow in this equipment for most of the liquids considered. Goldstein (19) in a discussion of the Reynolds criterion for flow between two parallel plates--one moving and one stationary--referred to a critical Reynolds number calculated by Orr to be 177 and stated that "These minimum criteria are well below the observed lower criteria." Presumably then the experimental values are of the order 300-500. Calculation of the Reynolds number for experimental systems may be made in accordance with the equation

$$Re = \frac{cVs}{z} \qquad (30)$$

where

c = clearance (low value) = 10 mils = $\frac{0.01}{12}$ ft,

V = rotor velocity (minimum) = $\frac{2\pi\ (1.75)(3600)\ \text{ft/sec}}{1216}$,

s = density in lb/ft^3, and

z = viscosity in $\frac{lb}{sec\text{-}ft}$.

Values of the Reynolds numbers for the experimental systems as calculated from equation (30) are given in Table 6. At the selected clearance of 10 mils, it would appear that turbulent flow might obtain only in the case of water. When the clearance is increased to 40 mils, however, then

Table 6. Reynolds Numbers for Experimental Systems[†]

	Viscosity (cp)	Density(g/cc)	Reynolds No.
Water	0.41	0.980	10,200
Mineral Oil	15.0	0.865	245
Paste No. 1	30.0	1.015	144
Paste No. 2	50.0	1.230	105
Paste No. 3	370.0	1.480	17.1
Paste No. 4	1080.00	1.470	5.8
Paste No. 5	>1000	1.330	<5.7

[†] c = 10 mils

turbulence might be predicted for all viscosities up to that of Paste No. 2. Thus, the Reynolds criteria as approximated in this case suggests the probability of flow transitions during the experiments with mineral oil, Paste No. 1 and Paste No. 2.

The probable occurrence of turbulent flow is also supported by the observation that power consumption is independent of the rotor clearance. This point may be made by an analogy with flow in pipes, in which case for streamline flow

$$F = 32\,\frac{zVN}{g_c s D^2} = \text{mechanical energy loss/lb flowing}$$

where z, v, N, g_c, and s may be regarded as constants, and since the weight flowing is proportional to D^2, therefore mechanical energy loss is independent of D, the pipe diameter.

In turbulent flow

$$F = \frac{2fV^2N}{g_c D}$$

and if the range of "Ds" under consideration are small enough, f may be taken as a constant along with the other factors, and the mechanical energy will be seen to vary with D to the first power.

Now in the case of streamline flow in the milling equipment, the analysis in Chapter II showed that power consumption should be inversely proportional to c, the rotor clearance. Then by analogy with pipe flow, it is reasonable to suspect that the power consumption for turbulent flow

should be independent of c, i.e., one power higher than in the case of streamline flow, thus being C° (c to the zero power). This would, of course, be in agreement with the experimental findings.

Additionally, the insensitivity of Δp to enormous variations in viscosity strongly suggests turbulent flow, since the equations for pipe friction show Δp to be proportional to viscosity in streamline flow but very insensitive to it in the turbulent region.

Finally, the nature of the fluid flow in the equipment may be indicated by relations between power consumption and viscosity. For streamline flow, viscosity is by definition directly proportional to the resisting force and, thus, to the power consumption. For turbulent flow, the resisting force will be approximately proportional to the 0.2 power of the viscosity for flow in smooth round pipes. This quantity is readily derived from the correlation of the Reynolds number with the Fanning friction factor. Comparison of these criteria with the experimental results was made using the equation

$$\frac{P_1}{P_2} = \left(\frac{Z_1}{Z_2}\right)^n. \qquad (31)$$

Substitution of experimental values gives

$$\frac{2.68}{2.01} = \left(\frac{30}{15}\right)^n$$

$$1.33 = 2^n$$

$$n = 0.41.$$

Thus the value of n again suggests that the flow is turbulent.

The experimental measurement of viscosity presents a particularly difficult problem. At the high shearing rates involved with the milling equipment, the relative viscosities of liquids are not likely to be the same as those obtained at low shearing rates in a viscosimeter. This is particularly true of pastes containing suspended solids. More extensive flow experiments together with rheological studies would undoubtedly lead to a means for empirical correlation, but such a project would be incidental rather than essential to the objectives of the present work.

To provide some guidance for initial mill settings in the actual operation of the equipment, an approximation method has been devised. When all of the experimental points (excepting those for Paste No. 5) are plotted on coordinates of $\underline{p}$ and $\underline{c}$, a definite trend is observed. Furthermore, when the specific correlations for Pastes No. 1 and No. 2 are re-examined, the expression for Paste No. 2 at $Q = 0$ is seen to define the general trend very well. This expression, based on equation (27), is

$$p = \frac{84}{c^{0.5}} \qquad (32)$$

The plot of all experimental points together with equation (32) is shown in Figure 20. For estimation of mill settings, the experimental points are usually more helpful than equation (32). The important consideration is that for a given rotor clearance, higher viscosities and higher flow rates require higher pressures, and conversely, lower viscosities and lower flow rates require lower pressures.

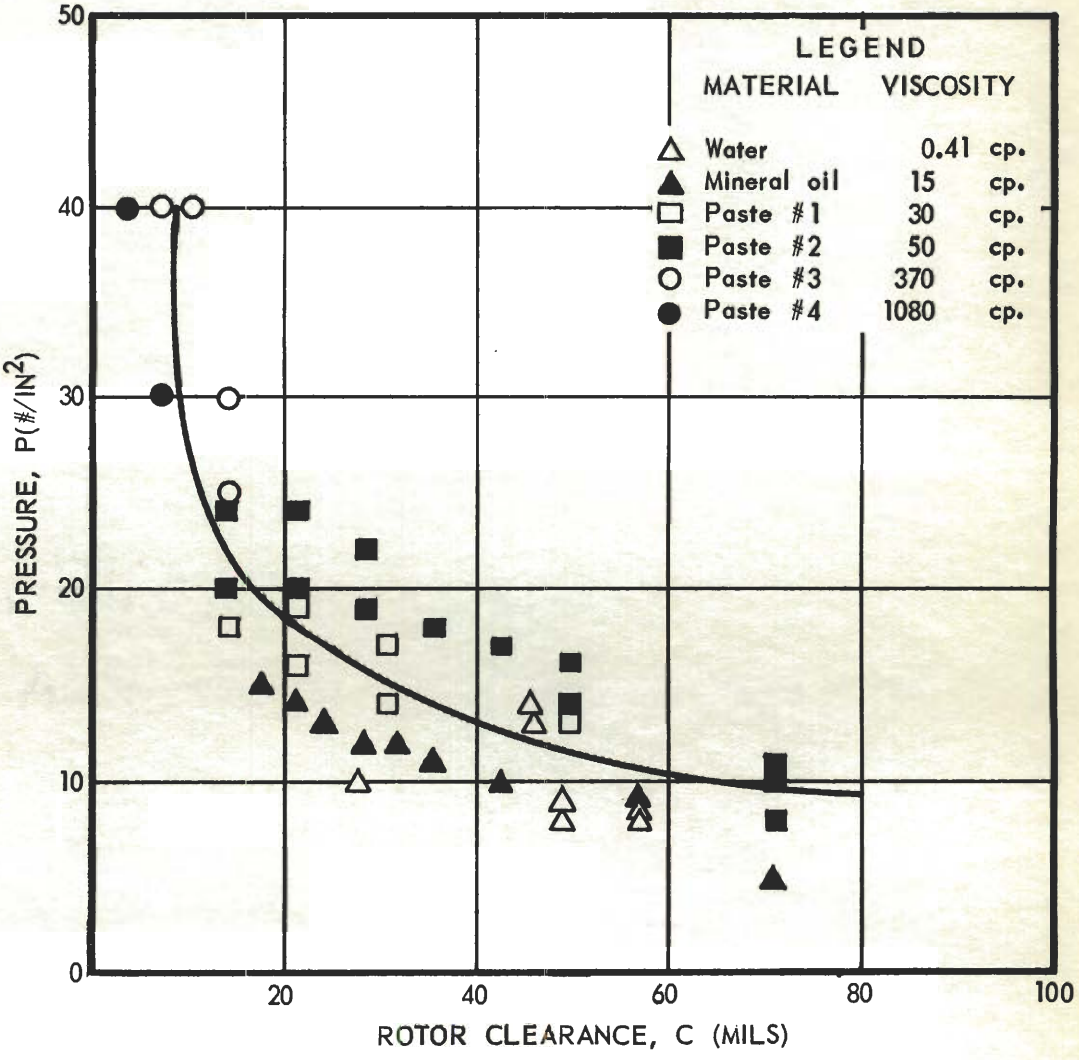

Figure 20. Pressure-Clearance Relations.

Power requirements.--A theoretical expression for power consumption was given in Chapter II, equation (1). The equation is applicable only to the power consumed in the milling zone under conditions of laminar flow. The experimental measurement of power consumption included all liquid effects on the rotor both in the milling zone and in the cavity above the rotor. Even if the "cavity-power" were accounted for, it is obvious that a correlation by the theoretical equation must be unsuccessful since the experimental data indicate that power is independent of rotor clearance for all of the conditions tested, while the equation requires that power be inversely proportional to the rotor clearance.

To check on the order of magnitude of the theoretical power as compared to the experimental measurements, equation (24) was evaluated for P as follows:

$$P = \frac{z}{c \times 1.03 \times 10^{3}}. \qquad (33)$$

When a typical value of c = 0.040 inch is selected, the comparisons are as shown in Table 7.

Table 7. Theoretical and Experimental Power

Fluid	z (cp)	Theoretical Power (hp)	Experimental Power (hp)
Mineral Oil	15	1.46	2.01
Paste No. 1	30	2.92	2.68

While the theoretical values are not absolutely correct, they are at least of the proper order of magnitude.

Original plans to measure power consumption on all experimental runs were precluded by a breakdown of power instrumentation. Nevertheless the information obtained was adequate for the purpose of this study, since it indicated clearly that in practical operating ranges power consumption is substantially independent of rotor clearance and is primarily dependent upon viscosity.

Dispersion effects.--Attention is directed to the compositions of Pastes No. 3, No. 4, and No. 5 as given in Appendix B and to the dispersion results as presented in Chapter VI, Table 3. Paste No. 3 was a white enamel formulation of a type usually described in the trade as an "architectural enamel". A minimum Hegman gage reading of seven is usually required for this type product. Paste No. 4, the house paint, should be dispersed to a Hegman reading of about four. Paste No. 5 was not representative of a specific product; but it is similar to the types of dispersions required for latex-emulsion paints, and a minimum Hegman reading of about four would be desired.

The viscosities of Pastes No. 3 and No. 4 were sufficiently high to allow the gear pump to produce adequate pressures. This permitted rotor clearances to be reduced to a position that was expected to have been sufficiently close to produce good dispersions. Values of three were the best that could be obtained with Pastes No. 4 and No. 5, and a value of only one was obtained with Paste No. 3. Furthermore, a second

pass through the mill for Paste No. 3 did not significantly improve the dispersion. Thus, the dispersion results obtained in this experimental study must be regarded as unsatisfactory.

Nevertheless, the poor dispersion performance cannot reasonably be interpreted as a complete invalidation of the theoretical principles previously set forth. Proper functioning of the mill is dependent on the ability of the mill to effect reduction of coarse particles to the requisite size simultaneously with internal classification action. Thus, if the dispersion function is inadequate, a resultant overcrowding of coarse particles in the milling zone may be expected to inhibit classification effectively. The actual flow pattern could be such that both dispersion and classification are inhibited. For example, if the angular velocity profile departs markedly from the straight line condition originally proposed, then a situation could exist in which centrifugal effects might be negligible in a comparatively thick zone adjacent to the stator. This would mean that coarse particles would not be removed from that zone, but would be passed through the mill without being classified or dispersed.

A possible solution to this problem might be to introduce high turbulence and impact effects in the milling zone either by fluting the milling faces with radial grooves or by substituting carborundum stones for the steel milling faces. Any tendency for channeling near the stator would then be eliminated, and dispersion effects would obviously be enhanced.

Another feature of mill performance that requires comment is the temperature of the pastes during milling. Many paint vehicles are heat-sensitive, and temperatures above 60° C would be prohibitive in these

cases. The present mill design is definitely unsatisfactory in this respect, and adequate water jacketing and means of reducing heat generation are needed. In fairness to the present mill, one should note, however, that the problem of heat generation has not been completely solved with any of the colloid-type mills used in paint manufacture.

CHAPTER VII

CONCLUSIONS

1. The colloid mill design investigated in this work embodies novel fundamental design features.

2. Theoretical hydrodynamic considerations support the principle of internal particle size classification as proposed.

3. Fluid flow experiments on the prototype mill indicate the possible occurrence of transitions of flow type in the ranges of normal operation.

4. A generalized flow correlation has not been developed, but sufficient data for guidance in mill operation have been obtained.

5. Dispersion experiments indicate that the mill (in the form tested) is generally unsatisfactory for the production of paint dispersions. Pigment dispersion is inferior to that obtainable with conventional high-speed stone mills, and the temperature rise in the paste is excessive.

6. The potentials of the mill design have not been fully evaluated in the present work. Operation at higher pressures and modifications of the surfaces of the milling faces--including the use of carborundum faces--represent additional investigations that should precede the formulation of final conclusions.

APPENDIX A

TABLE OF SYMBOLS

A	slant area
A	constant of integration
A	cross sectional area
a	outside radius of stator
B	constant of integration
b	inside radius of stator
c	rotor clearance
D	pipe diameter
d	particle diameter
d	differential operator
F	force
g	acceleration of gravity
K	a constant
K_c	centrifugal pressure constant
K_f	frictional resistance constant
L	settling length
l	slant height
P	power
p	pressure
Q	rate of flow
R	revolutions per minute

TABLE OF SYMBOLS (Continued)

r	a radial distance
s	density or specific gravity
T	temperature
T	time
U	total volume in the milling zone
u	linear velocity
V	circumferential velocity
y	a variable distance normal to stator face
z	viscosity

GREEK SYMBOLS

ω	angular velocity of the liquid
ω_R	angular velocity of the rotor
θ	angle of milling faces with the horizontal

APPENDIX B

FLOW EXPERIMENTS
Composition of Clay-Mineral Oil Pastes

Component	Percentage by Weight
Paste No. 1 (25% Clay)	
Mineral Oil (250 SAE)	69.58
Mineral Spirits	5.42
Clay (Velvacast-Ga. Kaolin)	25.00
Paste No. 2 (50% Clay)	
Paste No. 1 (25% Clay)	66.70
Clay (Velvacast-Ga. Kaolin)	33.30

APPENDIX B (Continued)

Composition of Paint Pastes

Constituents	Milling Batch (pounds)	Final Let-down (pounds)
Paste No. 3 - White Enamel		
Rutile TiO_2	10.20	
Zinc Oxide	3.93	
Magnesium Silicate	1.56	
Styrenated D.C.O.†	13.40	
Mineral Spirits	2.00	3.36
Driers		0.36
Pigment Content (% by weight)	45.0	
Specific Gravity	1.48	

Constituents	Total Batch (pounds)
Paste No. 4 - House Paint Paste	
Antatase TiO_2	10.00
Zinc Oxide	2.50
Raw Linseed Oil	9.40
Z-3 Bodied Linseed Oil	3.10
Pigment Content (% by weight)	50.0
Specific Gravity	1.47
Paste No. 5 - Aqueous Dispersion	
Calcium Carbonate No. 40	5.00
Clay - Velvacast	5.00
Water	15.00
Pigment Content (% by weight)	40.0
Specific Gravity	1.33

†Styrenated Dehydrated Castor Oil (Cook Paint & Varnish Co.)

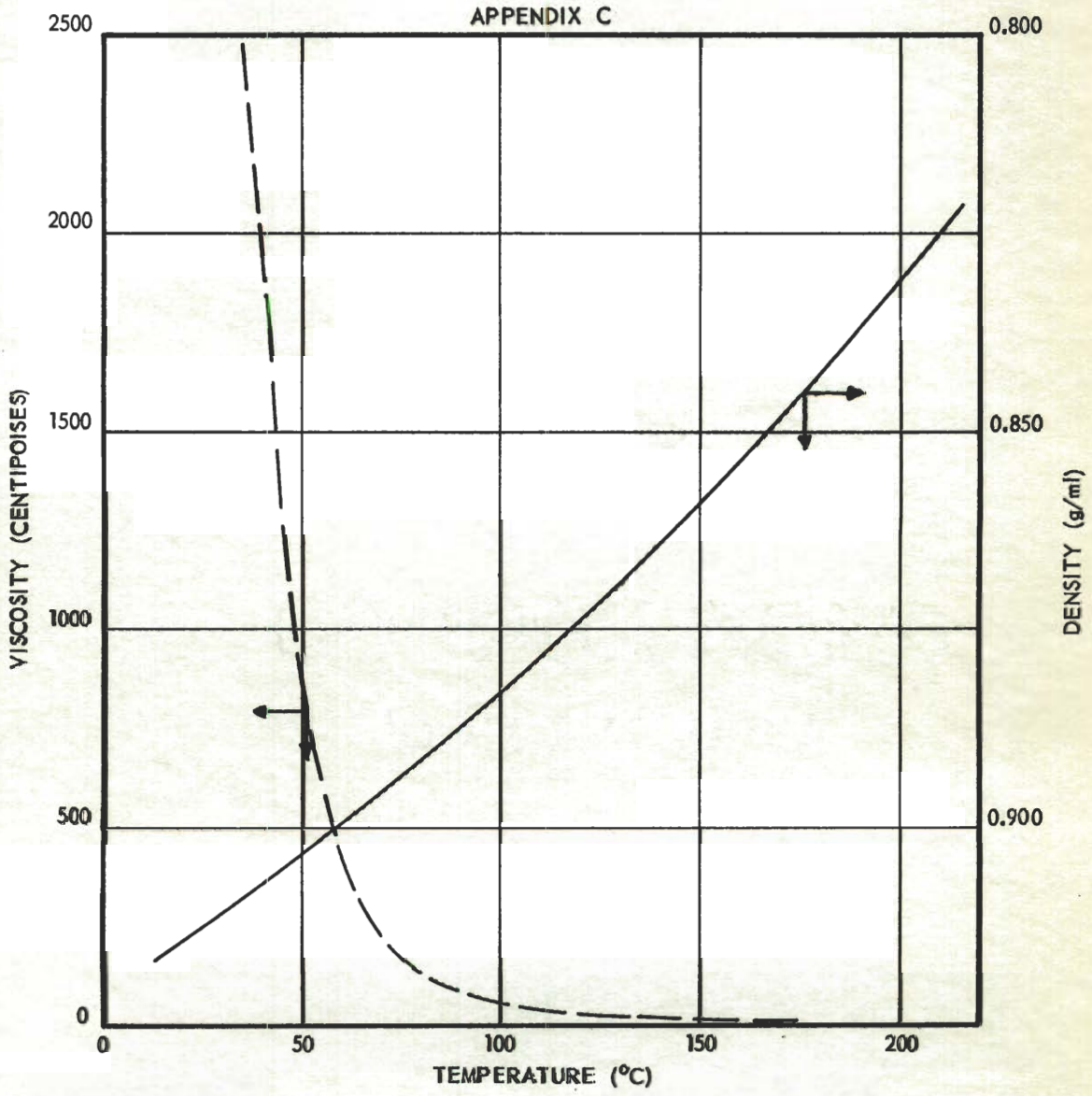

Figure 11. Density-Viscosity-Temperature Properties of Mineral Oil.

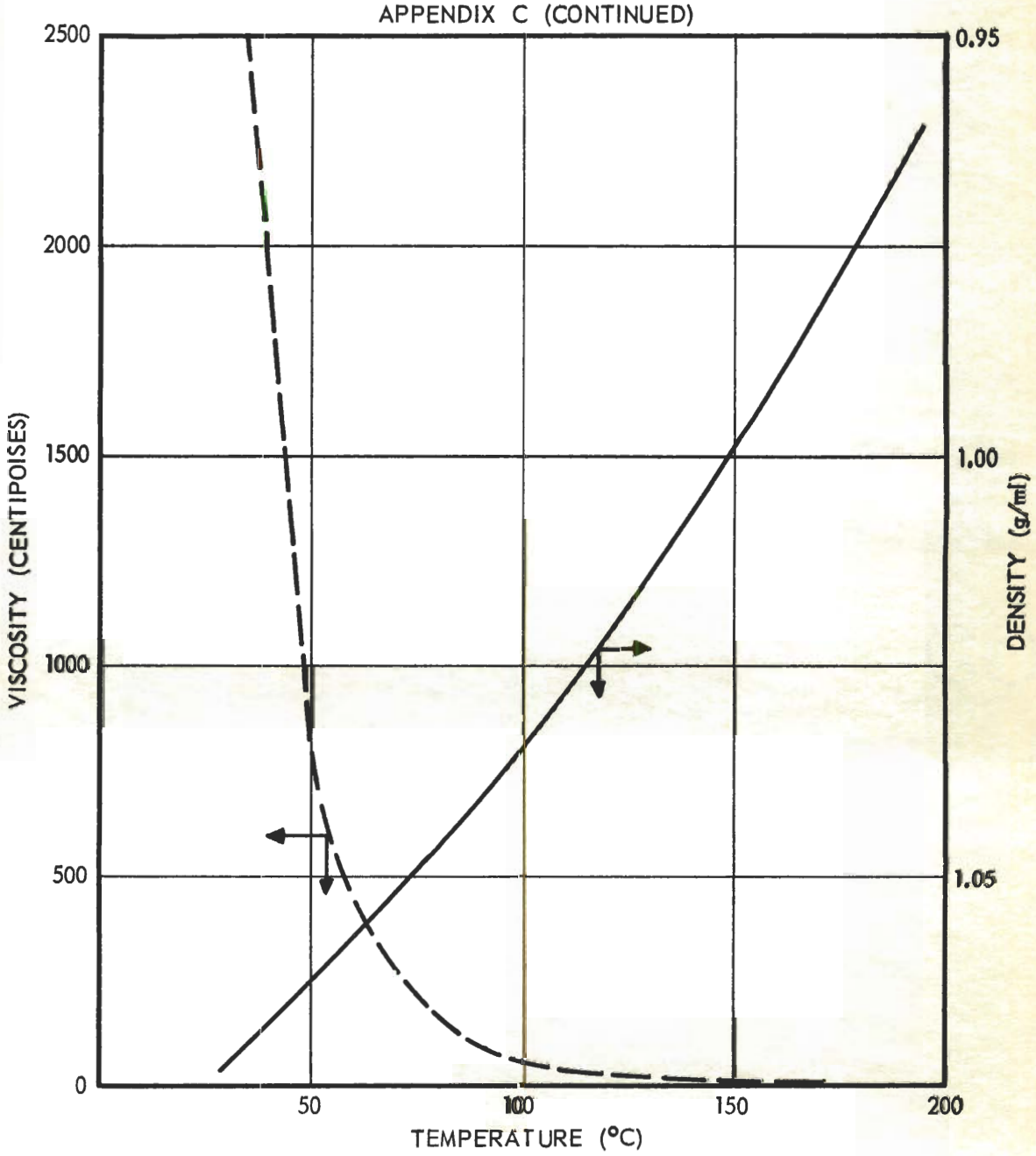

Figure 12. Density-Viscosity-Temperature Properties of Paste #1.

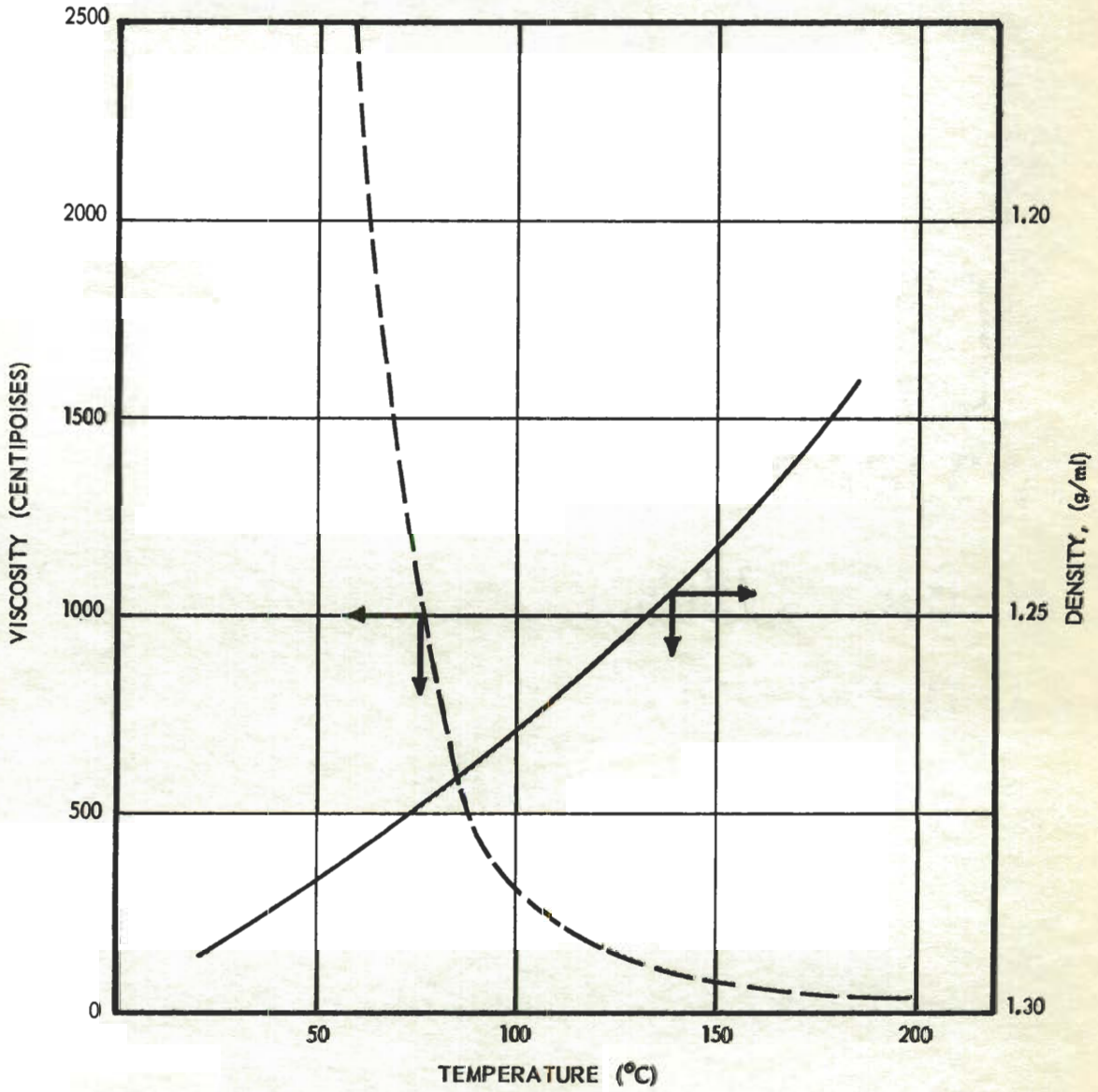

Figure 13. Density-Viscosity-Temperature Properties of Paste #2.

BIBLIOGRAPHY

REFERENCES CITED

1. Fischer, E. K., Colloidal Dispersions. New York: John Wiley and Sons, Inc., 1950, p. 56.

2. Harkins, W. D., and R. Dahlstrom, "Wetting of Pigments And Other Powders," Industrial and Engineering Chemistry 22 (1930). 897-902.

3. Perry, J. H., Chemical Engineers' Handbook, 2nd ed. New York: McGraw-Hill Book Company, Inc., 1941. pp. 1541-1560, 1917-1920, 1978-1980.

4. Fischer, op. cit., pp. 297-347

5. Bidlack, V. C., and E. W. Fasig, Paint and Varnish Production Manual. New York: John Wiley and Sons, Inc., 1951. pp. 37-42.

6. Foy, W. L., H. J. Pausing and W. A. Ziegler, "A Preliminary Study of Fine Pigment Dispersion on the Morehouse Mill," Official Digest of the Federation of Paint and Varnish Production Clubs, No. 322 (Nov. 1951). 751-757.

7. Taylor, J. J., "Fine Pigment Dispersion," Official Digest of the Federation of Paint and Varnish Production Clubs, No. 26 (1953). 445-455.

8. Anonymous, "Dispersing With Kinetic Energy," Paint and Varnish Production 43 (1953).

9. Shurts, R. B., "The Association New High Speed Stone Mill," The National Paint, Varnish, and Lacquer Association, Scientific Section, Special Bulletin, Oct. 1953.

10. Travis, P. M., Mechanochemistry and the Colloid Mill. New York: Reinhold Publishing Company, 1928. p. 148.

11. Von Weimarn, P. P., Grundzeuge Der Dispersoid Chemie. Dresden: Verlag Von Theodor Steinkopf, 1910. p. 82.

12. Plauson, H., See Reference 15.

13. Clayton, W., The Theory of Emulsions and Their Technical Treatment. Philadelphia: P. Blakiston's Son and Co., Inc., 1935. pp. 325-338.

14. Fischer, op. cit., pp. 338-346.

15. Patents Relating to Colloid Mills: Plauson, U. S. 1,500,845, 1924; Eppenbach, U. S. 1,728,178, 1929; Eppenbach, U. S. 1,738,288, 1929; Hurrell, U. S. 1,756,198, 1930; Soule, U. S. 1,764,760, 1930; Dawson, U. S. 1,807,773, 1931; Ostermann, U. S. 1,885,283, 1932; Ostermann, U. S. 1,885,283, 1932; Plauson, U. S. 1,923,013, 1933; Tolman, U. S. 1,927,620, 1933; Morehouse, U. S. 2,147,821, 1939; Morehouse, U. S. 2,296,564, 1942; Hofman, U. S. 2,321,599, 1943; Hofmann, U. S. 2,435,216, 1948; Shaw, U. S. 2,513,752, 1950.

16. Lamb, H., Hydrodynamics. London: Cambridge University Press, 1932. p. 581.

17. Baker, C. P., and J. F. Vozzella, "Evaluation of Production Club Fineness Gage," Official Digest of The Federation of Paint and Varnish Production Clubs, No. 311 (December 1950), 1076-97.

18. International Critical Tables 1st ed. Vol. 5. New York: McGraw-Hill Book Company, Inc., 1929, p.10.

19. Goldstein, S., Modern Developments In Fluid Dynamics, Vol. I. London: Oxford University Press, 1952. p. 195.